TÉCNICO LISBOA

Double-Sided Self-Pierce Riveting On Polymer-Metal Joints

Patric Teixeira Pereira

Thesis to obtain the Master of Science Degree in

Mechanical Engineering

Supervisors: Prof. Luís Manuel Mendonça Alves

Prof. Rafael Augusto Nunes Miranda Malta Afonso

Examination Committee

Chairperson: Prof. Rui Manuel dos Santos Oliveira Baptista

Supervisor: Prof. Rafael Augusto Nunes Miranda Malta Afonso

Members of the Committee: Prof. José Rui de Carvalho Mendes Marcelino

Eng. António José Ferreira Gonçalves Cartaxo

October 2021

Acknowledgements

To Professor Paulo Martins, Professor Luís Alves and Professor Rafael Afonso, I cannot express enough gratitude for the chance to work with you. Unexpectedly, for the first time in my academic and personal life I was able to find meaning and fulfilment in such a rewarding challenge and work. Thank you for providing me such a positive and inspiring experience as a conclusion to a journey mainly associated with struggles, doubts and fears. I would also like to acknowledge the enthusiasm and the way in general you welcomed me in this journey, providing me enough autonomy to freely explore, fail and especially learn along the way. Thank you to all three for upholding the true values a Professor should have.

To my mom and dad, I made it. I will soon be certified to switch lights bulbs around the house and fix broken cabinets, just like real mechanical engineers do, according to you both! I owe it to you. I owe everything to you. Thank you for the incessant support and trust. Thank you for the sacrifices you made that allowed me to choose and pursue my own path. Forever grateful, I can only hope that someday you will feel as proud of me as I am of you.

To my sister, I hate to admit it, but I have no choice! Thank you for your brilliant and intuitive mind, that despite not having a single clue regarding mechanical behavior of materials, was able to provide me relevant insights, ideas, and creative solutions during the development of this work. Thank you, also, for taking care of me during such a troubled period in my life. You mean the world to me, even when we are annoyed at each other.

To Andy, Mário and Daniel, I would like to thank you for being present and supportive not only through the restless nights spent studying, but also through the ones spent enjoying life. Thank you for making this journey much more meaningful and fun.

Abstract

Double-sided self-pierce riveting is a recently proposed new joining by forming technology. As the name suggests, this technology draws inspiration from the already well-established self-pierce riveting process and aims to provide an alternative solution for diverse applications due to its unique differentiation from already existing mechanical joining technologies in terms of inherent advantages and applicability.
Conceptually, double-sided self-pierce riveting consists in joining together two components by pressing between them a tubular rivet with chamfered ends on both sides through the action of a punch. The interaction between the solicited compressive force and the geometry of the rivet causes it to gradually pierce and flare through both materials, generating a mechanical lock between the components.
The main goal established for this thesis is to develop knowledge regarding double-sided self-pierce riveting by providing further experimental and computational investigation and analysis to the process and its key variables, while expanding its range of material applications to polymers and subsequently dissimilar polymer-metal applications. Additionally, given the potential demonstrated by the technology, this thesis aims to provide information and insights relevant to the process in terms of potential applications, optimizations, tooling and future development opportunities with the intent of validating and encouraging its industrial implementation.

Keywords

DSSPR, Joining by Forming, Polymer, Dissimilar Materials, Rivet, Sheet, Finite Element Modelling

Resumo

Double-sided self-pierce riveting, ou rebitagem autoperfurante dupla é numa nova tecnologia de ligação mecânica por enformação. Como o nome indica, esta tecnologia é uma variação da já existente rebitagem autoperfurante, e tem vindo a ser desenvolvida com o intuito de fornecer uma nova alternativa aos processos de ligação atualmente utilizados, dadas as vantagens únicas e intrínsecas ao processo.

Conceitualmente, a rebitagem autoperfurante dupla consiste no processo de união mecânica de dois componentes através da compressão de um rebite tubular entre ambos. A interação entre as forças compressivas associadas e a geometria característica do rebite promove a penetração e conjugação simultânea de um processo de expansão radial e dobragem consecutiva (*flaring*) do rebite, criando o bloqueio mecânico dos componentes.

O objetivo primário estabelecido para este trabalho consiste tanto na expansão do conhecimento já adquirido acerca da tecnologia em termos de variáveis geométricas e processuais, como também na expansão da aplicação da tecnologia a materiais poliméricos e a ligações de materiais dissimilares polímero-metal, recorrendo à realização de estudos experimentais e de modelação de elementos finitos. Adicionalmente, motivada pelo elevado potencial de aplicação demonstrado por este novo processo, esta tese pretende proporcionar uma visão detalhada de otimizações ao processo e eventuais conceitos de aplicação, da viabilidade económica e ferramentas requeridas, e finalmente de perspetivas de futuros desenvolvimentos e estudos desta tecnologia, com o objetivo de validar a sua implementação industrial.

Palavras-Chave

DSSPR, Ligação Mecânica por Enformação, Polímero, Materiais Dissimilares, Rebite, Chapas, Modelação por Elementos Finitos

Index

Lists of figures

List of tables

1.Introduction

Pressured by the present fast-paced technological modernization period fueled by environmental and socio-economic challenges, the industrial sector is actively shifting and seeking new solutions and technologies capable of responding to present demands and requirements. Consequently, a growing in innovation, developments, and introduction of new materials to most industries, as well as the adaptation of existing materials to novel applications increased the need to develop technologies capable of handling such variations. Parallel to this, development needs equally grow in the technologies that come with industrial manufacturing, namely joining technologies.

This thesis is therefore focused in extending both the knowledge and the application range of double-sided self-pierce riveting, an innovative mechanical joining technology, by studying its implementation in commonly used materials and material combinations presently used. The interest in extending the development of this technology was fueled by the promising outcomes generated in initial studies. Characterized as a joining by forming process, double-sided self-pierce riveting presents itself as an appealing alternative to existing mechanical joining technologies like self-pierce riveting or clinching, providing comparative performance behaviors with inherent benefits that could better serve certain industrial applications.

By further investigating double-sided self-pierce riveting, this thesis provides enough advancements in the joining technology to assert its benefits and challenges, to ultimately seek its industrial implementation as a compelling, efficient, and effective alternative to current joining technologies. Given the early stage of development of the technology, the driving proposition of this thesis was to expand its range of applications in terms of materials to be joined, initially to polymers and later in dissimilar materials with very different mechanical strengths, to provide a proof of concept while simultaneously differentiating it and highlighting its main advantages from well-established joining technologies.

Nonetheless, work and analyses conducted were carefully and intently adjusted to ultimately pursue the industrial implementation of double-sided self-pierce riveting by experimenting potential variants that could benefit both the joint performance and its application.

Concerning the structure of this thesis, a the state-of-the-art chapter is presented, where the contemporary state of the industrial sector in terms of existing joining technologies is discussed in detail, and double-sided self-pierce riveting is presented to frame its development motivation, describing previous work published on the technology to date, which allowed to establish the base knowledge and investigative procedures associated with it. Chapter 3 aimed thereafter to describe in greater detail the experimental and numerical modeling procedures, which were followed accordingly during the development of the main body of work and investigation carried.

The second segment of the thesis contains the main body of the work, presenting firstly the study in polymer sheets, in chapter 4, and culminating in the study of joining polymer-metal dissimilar material sheets in chapters 5 and 6. Justified by the different the objectives and results associated with each material combination studied, results and respective discussions are presented independently in each corresponding chapter, aiming to provide the reader a better and faster understanding of how the process and the investigation carried affected the produced outcomes for each specific setting.

The last segment of the structure targeted the industrial implementation context of the main work developed during this thesis, embodied in chapters 7,8 and 9. In the referred chapters, information pertaining potential applications, equipment and tooling, costs and perspectives of future wok is provided.

A short conclusion is also presented and aims to summarize and compile the results gathered in all studies, while also providing an overall view regarding double-sided self-pierce riveting, its advantages, and its further development.

2. State of the art

As time and technology progresses, the automotive industrial sector struggles to find breakthrough technological advancements capable of retiring conventional and well-established processes and techniques. The modern industrial paradigm excels therefore by maximizing the potential of these conventional processes by improving and extending their efficiency, efficacy, range of applications and economic competitiveness. In a society mainly driven by capitalism and socio-economic growth, the modern automotive industry illustrates this phenomenon to a certain extent, since in recent years, cars did not fundamentally suffer major changes to how they work or how they are built. Instead, car manufacturers focused most of their efforts in designing faster, lighter and more efficient alternatives that meet quality standards, while reducing the overall associated costs, with the intent of increasing market shares, competitiveness and profits in the sector. These performance results were the direct effect of the aforementioned focus in the improvement of manufacturing techniques and technologies as well as the introduction of new materials to face the increasing costs of raw materials and energy [1].
A noticeable improvement in vehicle technical performance was achieved by the consolidation and improvement of the joining technologies and processes involved in a car's assembly manufacturing stage. The industry currently holds available to use various extremely precise, well defined and efficient joining processes capable of meeting the highest quality standards. Process automation and robotization proved to be a key improvement to joining processes and its implementation was possible through the knowledge acquired for decades and implemented in joining technologies, from welding to mechanical joining.
Welding represents one of the most productive joining processes available to the automotive industry ever since it was introduced. Techniques like gas metal arc welding and more recently resistance spot welding (RSW), schematically depicted in Figure 1, soon were presented as the most effective, economic, and best performing methods to join the steel-based body-in-white of cars. Resistance spot welding specifically, is a welding process that relies on heat generation by electrical resistance to current passing between two electrodes and through the metallic components to be welded. The interface of the materials, as the region of greatest resistance, melts due to an increasing heat generation, forming a weld nugget that bonds both materials permanently [2]. This process results in a sound joint with no overall weight impact, with the weld nugget protected between the overlapped sheets. However, as new materials were introduced to car manufacturing, an increasing need to join dissimilar materials (from different metallic materials to polymers) often deemed RSW as unreliable, due to the incidence of hard and brittle intermetallic compounds in the weld and due to the incompatibility related with the materials. One other limiting factor was associated with the thermal cycles suffered by the materials during the process, which would result in building residual stresses and distortions.

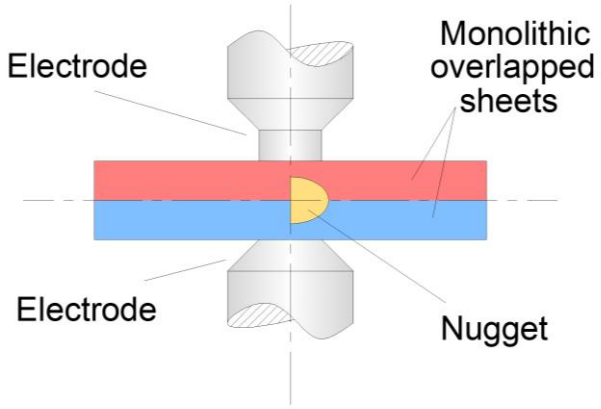

Figure 1. Resistance Spot Welding of sheets.

Given the limitations common to the welding processes discussed above, other joining technologies were also introduced to car manufacturing. In fact, even before welding was implemented, most of a car's assembly was performed by mechanically joining parts with processes like solid riveting and screwing. Since then, and given the trend of more diverse material usage, these technologies were refined and innovated to match quality standards and costs with welding processes. Joining by forming specifically, established itself as a viable technological alternative to RSW. It is defined as a technology that involves processes that permanently join materials by plastic deformation [3]. Among these processes, the most commonly used in the auto industry currently are self-piece riveting (SPR), clinching and flow drill screwing.

Flow drill screwing is a thermomechanical process of fastening two overlapped sheets characterized by three stages. The first stage uses high rotational speed of the screw to pierce the upper sheet, subjecting it to a temperature increase and high plastic strain associated with friction conditions. The second stage consists in forming an extrusion in the lower sheet. As the point of the screw pierces the lower sheet, its thread forming region creates a thread in the sheet and in the extruded boss, finalizing the third stage of the process. The screw is then tightened in a way that ensures enough clamp load without compromising the joint [4]. This process allowed therefore to offer a solution and application in cases where welding processes would not be viable, for example in composite material joints. Besides that, this process improved over regular screwing, since it allowed for the joint to be done with only one accessible side without any type of pre-drilling or pre-positioning of the screw, while still allowing the joint to be replaced or removed in a product's end-of-life. Although this process solves the challenges faced by other joining means with similar cost efficiency, it also has its own limitations and liabilities. F. Aslan et al. [5] demonstrated that the combination and interaction between the material's mechanical behavior and the process's driving parameters are critical to avoid characteristic defects and the underperformance of the joint, suggesting a high sensitivity of the quality of the joint to key parameters. Clinching is another cold-forming process and is currently one of the most used joining technologies available to the automotive industry since it allows a sustainable use of resources given the modern design criteria for industrial products associated with lightweight structures and even a certain range of

dissimilar material structures. Besides, it is a relatively simple process regarding its interlocking mechanics with equally simple implementation and tooling design allowing the process to be extremely flexible, adjustable, and cost effective while still guaranteeing comparable results in terms of joint integrity to other competing processes. Clinching was firstly implemented in 1985, having since then been studied, developed, and improved upon, validating its use over the well-established welding processes. Round clinching is the most common implementation for this process and is characterized by the use of a circular punch and die to plastically deform two overlapped sheets, creating a mechanical interlocking. The mechanical integrity of the joint is thereby determined by the degree of interlocking achieved, which can be adjusted by processual and tooling parameters accordingly. The process does have however certain limitations associated with its mechanical properties. The success of the interlocking is heavily affected by material selection and geometry of the sheets to be joined, and modifications to the process may have to be introduced in order to overcome such limitations [6]. For this reason, clinching may be economically impracticable and even impossible in some applications where DSSPR may excel, for example in the joining of thick plates.

Self-pierce riveting [7] is yet another popular joining technology used in the industry. This process saw great developments and applications since the end of the 20th century, becoming a great alternative to any other processes mentioned above. It is also categorized as a cold-forming process, where a tubular rivet is punched through two overlapped sheets. As the rivet pierces the sheets, it flares along with the assistance of a die generating the interlocking between the components. The process is therefore characterized by a piercing stage and a flaring stage, and can be described by the following four steps: Clamping, where a perpendicular force is applied by the punch to the rivet, pressuring the sheets between it and the die; Piercing, where the rivet is pushed through both top and bottom sheets by the action of the punch; Flaring, associated with material from the bottom sheet flowing along the shape of the die with a respective flaring of the skirt of the rivet, which generates the interlocking; Releasing, where the punch is released and the materials undergo elastic recovery. The advantages reached by this process are comparable to those from clinching, including the ability to join dissimilar materials to a greater range, with simple tooling without requiring any surface preparation at costs. The same extrapolation can also be made regarding the negative aspects and disadvantages for this process, as it is also limited by the mechanical behavior and geometry of the components, the order of placement of the materials and the degree of interlocking achieved. One other disadvantageous factor particularly relevant regarding SPR is related to effects the piercing stage has on the upper sheet, as the tearing of the material embrittles the surrounding area which compromises the quality of the joint. For this reason, this technology is also limited by the ductility of the materials to be joined.

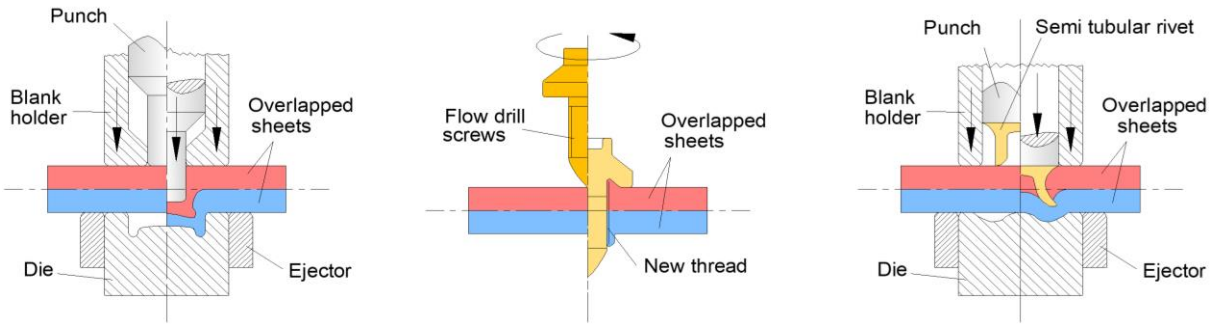

Figure 2. Mechanical joining processes: a) Clinching; b) Flow drill screwing; c) Self-pierce riveting.

As the industry evolved, the complexity of the components to be joined as well as the increasing performance requirements and quality standards forced the typically used processes like the ones described to adapt to each specific circumstances. Continuous investigations regarding these processes soon enabled the use of different kinds of variations and combinations that allowed the extension of the range of applications for all processes. As an example, the process of traditional clinching currently has a vast list of variations associated with it like hole-clinching, electromagnetic clinching, and injection clinching to name a few. The same can be said for self-pierce riveting, where variants like friction SPR and hydro-SPR are available [3].

Not only were these processes manipulated independently, but an emerging trend of combining two of them simultaneously became the norm associated with high-quality joints. These combinations became known as hybrid joining technologies, and allowed the combined processes to complement each other, overcoming limitations that would exist otherwise. A particularly common hybrid joining process used in the automotive industry involves the use of adhesive bonding to complement a process like SPR or clinching. Adhesives by themselves, although they may serve many applications, often fail in cases where peeling loads or tension loads are applied, as well as in cases associated with thermal cycles which causes adhesion or cohesion failures of the joint. The process is also relatively difficult to control since surface preparation and adhesive quality may impact the curing process and consequently the structural integrity of the bond. Even though this process is limited by its properties, it allowed great developments in the applied products by having a significant impact in weight reduction of structures, while improving durability at an extremely competitive manufacturing cost. For this reason, adhesives became a particularly popular joining technology to complement mechanical joining processes, allowing an improvement not only in the mechanical behavior of the joint, but also in the water-tight seal formed responsible for a reduction of possible corrosion effects [1].

As discussed above, recent efforts in innovation aimed to adapt and complement existing technologies to increase their range of application or reduce their limitations. Following that scope, Alves et al. [2] proposed and developed an alternative process, designated as “double-sided self-pierce riveting” (DSSPR in its abbreviated form). The attributed name derives from the previously discussed SPR, as it is a variation of this process, sharing to some extent its mechanical and technical fundaments and principles. Initially proposed in a paper by Kato et al [8], the authors described this joining by forming

process as the connection of two sheets through means of a tubular shaped rivet pressed between them, through the action of a punch. Similar to the flaring stage of SPR, the tubular rivet is designed in such way that as the punch squeezes the sheets together, penetration and flaring of the rivet occurs, generating a mechanical interlocking. This process development was mainly motivated by the discussed limitations SPR currently faces. In that sense, the authors concluded that through the implementation of DSSPR, it is possible to join sheets of larger thicknesses as the process does not depend on sheet geometry and is also possible to join an increased range of dissimilar materials, since there is no sheet piercing affecting or generating brittle structures. In addition to tackling these main disadvantages associated with SPR, double-sided self-pierce riveting also inherits new benefits compared to the mechanical joining processes currently available. Given the fact that the rivet is pressed between the overlapped sheets, the joint formed is invisible and inaccessible, which is not only relevant from an aesthetic point of view but also limits the effects of galvanic corrosion, with no kind of material protrusion being generated. Secondarily, simple rivet geometry and simple tooling requirements imply lower overall costs associated with the process, making it a serious candidate as an alternative to current industrial applications.

As previously mentioned, double-sided self-pierce riveting is characterized as a cold forming process in which a tubular rivet is pressed between two sheets through the action of flat parallel punches, generating a mechanical interlocking of both sheets as a result of plastic deformation in the form of flaring of the rivet, as shown in the figure below. From the conceptual definition, in the first published paper regarding the topic [2], the authors pursued a complete definition of the process in terms of geometric parameters and variables.

DSSPR can be separated in two major components: the tubular rivet and the sheets (Figure 3). While both parts may vary along the course of development, the geometrical variables are inherently present throughout the studies and were duly identified.

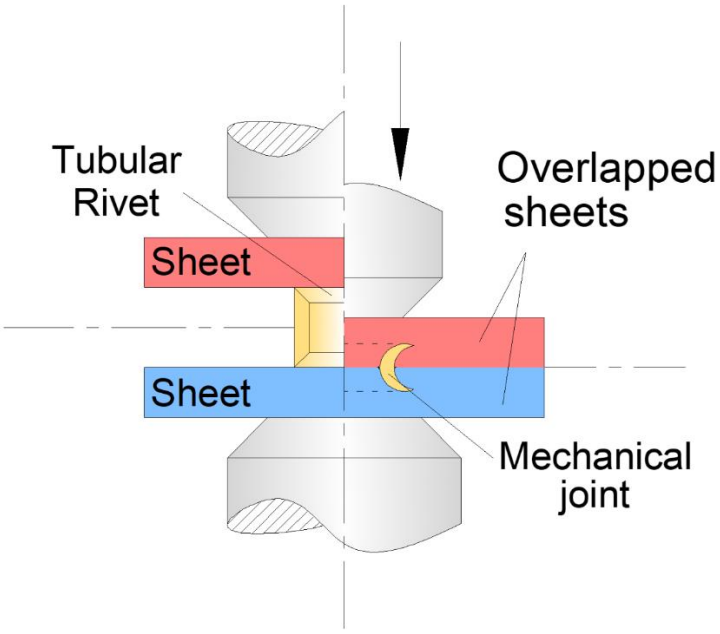

Figure 3. Schematic representation of a cross sectional joint produced by DSSPR before (left) and after (right) joining.

Regarding the rivet, geometrical variables were established for both of its undeformed and deformed states to correlate the undeformed geometric variables to the amount of flaring, and consequently to the reliability of the joint obtained. Concerning the undeformed state of the rivet (Figure 4a), the main geometric features identified consist of the initial height (h_0), the outer diameter (d_0), the wall thickness (t_0), and the chamfered angle (α). As regards to the deformed shape of the rivet (Figure 4b), three variables were identified, namely the outer diameter (d), the final height (h) and the interlocking distance or undercut (i). The last one is particularly relevant for the performance analysis, as it is a direct indicator of the mechanical resistance of the joint, given the intuitive direct correlation between the interlocking distance and the amount of force required to destroy or separate the joint.

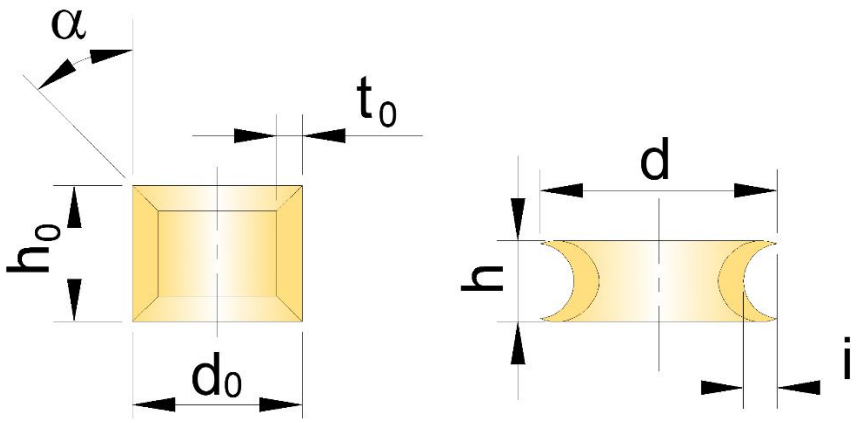

Figure 4. Rivets used in DSSPR: a) Schematic representation of geometric parameters; b) Rivet samples.

Finally, the pair of sheets geometric parameters are relatively simple, as they are only characterized by their thickness, length, and width. During the course of the work developed, these parameters remained constant, as the main scope of the study was only to identify the influence of the rivet's geometry (Figure 4a). There was however a geometric feature introduced to the sheets in a later stage of the work, where a flat-bottom hole with a specific depth and diameter was drilled to one of the sheets. The purpose and characterization of this feature is later introduced in the chapter pertaining dissimilar materials.

In terms of results gathered from the initial study in metal sheets [2], the authors successfully identified the main deformation modes and mechanics involved in DSSPR.

The sensitivity tests regarding initial chamfered angle (α) variations allowed to conclude that the amount of flaring obtained was a direct function of that angle, as higher angles translated in lower interlockings (refer to Figure 4) and consequently a worse mechanical strength of the joint. The results also proved that the initial height (h_0) of the rivet had a significant impact on the interlocking between sheets, as increasing the initial height increased the amount of interlocking achieved, although this trend was limited by the height's critical value associated with an instability of the rivet. These influences set the

specific range of sensitivity of the variables, since values outside this range would not benefit the joint produced or its feasibility.

This study successfully validated DSSPR as an effective mechanical joining technology by consistently producing reliable joints. From the results gathered, a better understanding concerning the governing deformation mechanics involved and the impact of the geometric variables in the result was acquired. In terms of performance, the destructive tests suggested that the produced joints sustained load solicitations consistently comparable to existing solutions currently available like Clinching and Self-Pierce Riveting.

The gathered performance data and the observed absence of material protrusions, invisibility of the joint, geometric simplicity of the rivet and tools used expanded the potential of DSSPR and its industrialization, which motivated further investigation on the technology and its application on polymeric and dissimilar polymer-metal combinations.

3.Experimental work description

The experimentation process consisted of four main stages that were maintained throughout the different studies. The first three stages relate to the experimental procedures and consisted of component manufacturing, joining testing and destructive testing. The fourth stage consisted of numerical modelling procedures. Each stage is presented in detail below.

3.1 Component manufacturing

The components used in all the test samples were manufactured from the raw materials available for the study and involved relatively simple operations. Nonetheless, manufacturing of the rivets soon proved to be the most challenging step, despite their geometrical simplicity, mainly because of the manufacturing tools available.

The rivet manufacturing was fully performed on a semi-automatic lathe and began with cutting sections of a steel tube down to the designated rivet height (h_0), followed by the machining of the chamfered angles on both ends of the rivet with the desired angle (α). To obtain these angles, a drill bit was mounted to the lathe's tailstock assembly and pushed against the rivet fixed to the chuck while rotating. This technique offered some productivity at the cost of low precision. Additionally, the relatively small gripping area of the rivet to the chuck and the length and setup of the drill bit provided very low rigidity to the system, often generating wobbling defects on the machined angle. To counteract these issues, a clamp was manufactured to improve the tightness between the rivet and the chuck and ultimately to increase the system's rigidity. The solution implemented proved to be effective, and even though the degree of precision and tolerancing of the finished rivets was not ideal, the results were deemed acceptable for the application. Figure 5 shows examples of rivets manufactured and used in joining tests.

Regarding the sheet samples (Figure 6), the process simply involved cutting down sheets of raw material to the required dimensions using a hydraulic shearing machine. Regarding the destructive tests, more specifically the peel tests, an additional operation was performed where the samples were bent at a 90º angle using a hydraulic bending machine. This operation caused some complications when applied to PVC sheets, causing cracks in the material along the outer bent area. However, this complication did not compromise the tests and subsequent results, since the separation (and therefore, failure) occurred in the joining region as expected.

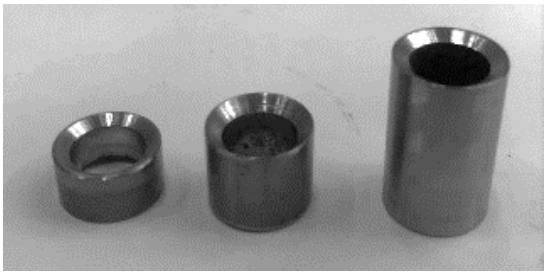

Figure 5. Manufactured rivets with different chamfered angles and initial heights

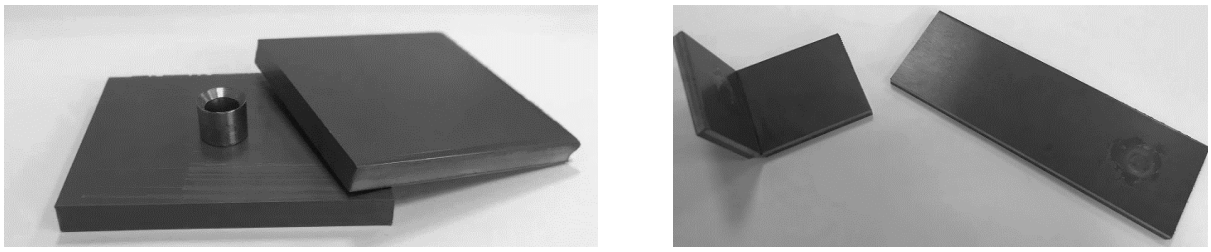

Figure 6. Sheet geometries used in joining tests (left) and destructive tests (right)

3.2 Material characterization

Experimental tests carried out in this work made use of three distinct materials. Two of the selected materials were used and characterized in the previous study of DSSPR [2], consisting of AISI 304 stainless steel for the rivet and AA5754-H111 aluminum for the sheets. Additionally, Polyvinylchloride (PVC) sheets with 5 mm thickness were used, and the material was characterized in a following paper pertaining DSSPR of polymer sheets [9].

Regarding the PVC, only the flow curve in compression was determined by means of a stack compression test [10], conducted as described in [9]. The flow curve in tension of the polymer was not characterized, as DSSPR is mainly driven by compressive stresses as concluded in previous developments.

The flow curves of these three materials are presented below.

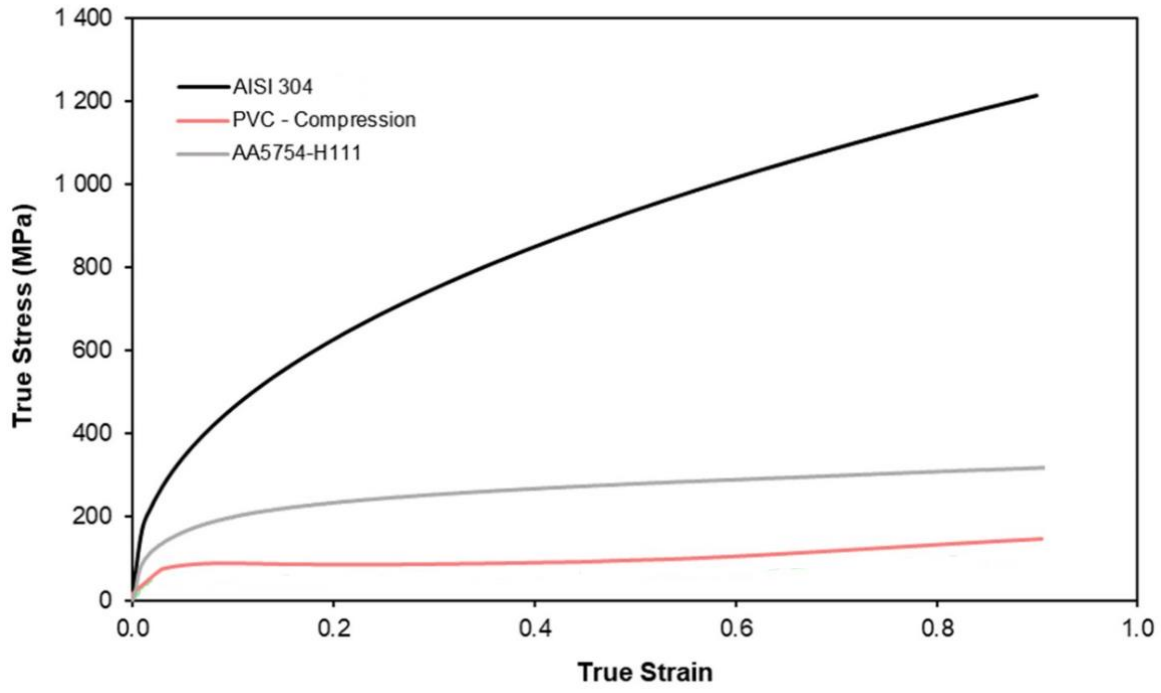

Figure 7. Stress-strain curves of the AA5754-H111 and PVC sheets and of the AISI 304 stainless-steel rivets.

3.3 Joining tests

The joining tests consisted in applying the riveting process with the intent of analyzing the progression and interaction between the materials and the compression loads involved in the process during the vertical displacement. These tests also carried the purpose of visually inspecting the joint externally and internally as posteriorly described.

To perform the tests, the hydraulic testing machine Instron SATEC with a load capacity of 1200 kN was used (Figure 8). The images on the center and right side show the compression platens used to perform the tests, and an assembled test setup, respectively.

Figure 8. Instron SATEC hydraulic testing machine and setup used in joining tests.

Considering the loads and displacements involved, as well as the precision required in the tests conducted, the friction between moving components and the elastic deformation of both the hydraulic machine components and the tools needed to be taken into account. To that purpose, an isolated compression test in-between platens was performed, from which displacements associated with the mentioned effects were gathered. This data was compiled into an elastic compensation curve (Figure 9) that relates the amount of elastic displacement according to the requested load. This curve allowed the adjustment of the following test results to obtain the desired accuracy, using an approximated 6^{th} degree polynomial equation, and the correspondent vertical displacement was subtracted for each one of the test results.

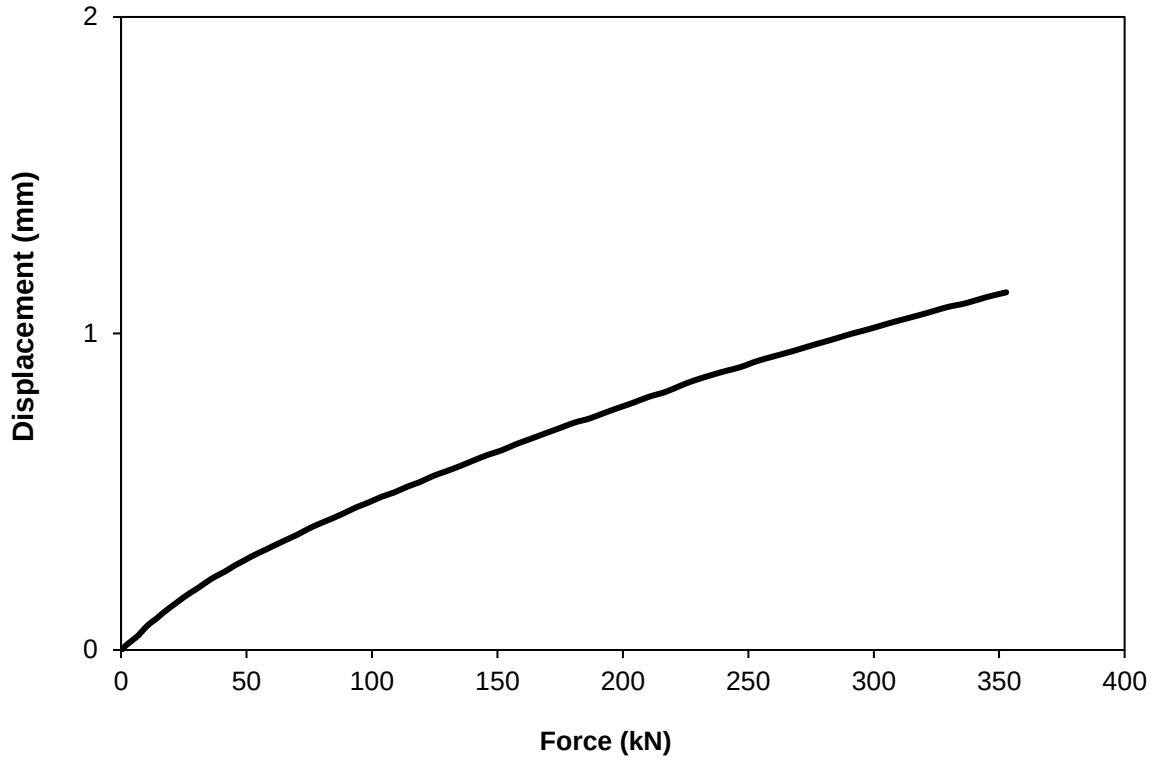

Figure 9. Elastic compensation curve of hydraulic testing machine

To finalize the tests, the samples created underwent a visual inspection to identify potential superficial defects and clearances and were then subjected to a cross-sectional cut by means of a band saw. The revealed cross-sections allowed further visual inspection and measurement of variables associated to the deformed rivet such as the interlocking distance (i), for a better understanding of the influence of the tested parameters in the resulting joint.

3.4 Destructive Tests

Shear and peel destructive tests were performed during the development of this work. These tests aimed to assess the joint's ability to withstand such conditions, as these types of forces are the most common and susceptible to destroy or separate the joint during its service life. These tests were carried in an Instron 5900R testing machine (Figure 10a) programmed to perform traction experiments. The testing setup as shown in Figure 10, consisted of a pair of tensile grips that allowed a rigid fixture to the test specimen.

Providing a shear effect to the joint was achieved by following standard ISO 12996 [11] and by applying the machine's tensile load in the direction parallel to the sheet's length, so the specimen only needed to be designed to have enough surface area to allow a good clamping grip that would not interact with the joint (Figure 10b).

The peel tests depicted in Figure 10c followed standard ISO 23598 [12] and the tensile load is applied perpendicularly to the longitudinal direction of the sheets and with an offset relatively to the rivet's central axis to generate the desired peeling effect.

a) b) c)

Figure 10. a) Instron 5900R testing machine; b) Shear testing setup; c) Pull-out testing setup.

3.5 Numerical Modeling

Numerical modelling had a crucial role regarding the advancements made in the DSSPR technology and the experiments conducted, as the finite element analysis provided a more comprehensive understanding of the deformation mechanics internal to the process by supplying processual field variables such as velocities, strain rates and others. Additionally, the finite element analyses performed allowed the reproduction of a comparative framework that established higher reliability to experimental results obtained. As a result of this framework, numerical modelling also served as a predictive tool for a more efficient organization of the experimental work performed, by identifying potential adjustments, improvements, and ineffective solutions to the joining process.

These analyses were carried out using *I-FORM 2D*, a bidimensional finite element computer program that utilizes Markov's principle of minimum plastic work rate, to account contact between deformable objects and incompressibility of velocity fields. Following this principle, the software is based on the finite element flow formulation, which is built upon the weak form of the quasi-static force equilibrium equations modified to include contact and sliding with friction between deformable objects, as portrayed by Alves et al in [2]. A more comprehensive description of this principle and its implementation in *I-FORM* is given by Nielsen et al [13].

I-FORM 2D is composed of three user interfaces designated as PRE, POST and REMESH, and an executable interface that runs the simulations. The PRE interface was designed to implement the initial conditions of the numerical simulation, from geometrical to process parameters. The REMESH interface allows for the user to perform remeshing operations, allowing for rectifications on process variables and elements, as well as mesh refinements. The POST interface serves as an analysis tool for the simulations since it grants access to visual and graphical inspection of the simulated process.

The setup for the simulations began by constructing the geometry of the components involved including the tools, according to the experimental case being studied. Then, materials were selected and assigned to each respective body. This selection provided the software information regarding mechanical properties and behavior of the materials required to perform the numerical modelling, including the elastic and plastic data, and density. The materials assigned to the rivet and polymer sheets were selected from the existing I-*FORM 2D's* database, while the material properties assigned to the aluminum sheets were obtained by inputting data from a stack compression test and a tensile test performed during a previous work [14]. The platens generated to perform the compression were approximated to rigid bodies discretized by linear contact-friction elements.

Friction was modelled according to the law of constant friction $\tau = mk$, where m is the friction factor and k is the flow shear strength. A friction factor of $m = 0.1$ was assigned to all object interfaces and this value was determined by comparing the estimated forces involved in the simulations with those verified in the experimental results.

A relevant optimization to the run time of the simulations was made by making use of the symmetry conditions of the cases studied. For the cases of similar material simulations, rotational and longitudinal symmetry was considered, therefore allowing for a reduction of the number of elements by 75%, while

in the cases of dissimilar materials a reduction of 50% was achieved by implementing the rotational symmetry condition.

Regarding the meshing process, the number of elements used and the number of remeshing operations presented a very high variability associated with large distortions of elements, and software limitations in processing deformations and contact boundaries between objects, particularly for the cases where polymer sheets were used. For this reason, several local and global remeshing operations were performed, where adjustments to the discretization of meshes and to the time increments were made to balance the run time and quality of the simulation. To quantify the mesh parameters, the table below presents the average numbers associated with mesh conditions according to each general case study.

Table 1. Average number of elements used in initial iterations and after remeshing operations.

	Initial number of elements	Number of elements after remeshing operation
Metal sheets	800	7000
Polymer sheets	3000	7500
Dissimilar materials	3000	10000

4 DSSPR of polymer sheets

Following the promising results of the previous initial study in metallic sheets [2], efforts were directed at assessing the range of applications regarding the sheets' materials. Based on that premise, the study aimed to assess DSSPR in polymers [9].

4.1 Testing parameters description

The battery of tests performed in this study had the goal of acquiring a comprehensive understanding of how the geometric variables of the rivet identified in the previous study [2] affected the joint when applied to polymers.

The first challenge emerged immediately at this stage, as a new geometric parameter had to be introduced to the rivet in the early stages of testing. This parameter consisted of a chamfered fillet radius r_f, a feature added to the chamfered angle α, to which a fixed value was assigned throughout the course of this case study. The necessity of introducing this parameter surfaced after verifying that this feature would improve the flaring effect and consequent interlocking generated, as explained in the next section. The tables presented below display the conditions under which the experimental and numerical works were developed.

Table 2. Geometric characterization of PVC sheets

PVC Sheets	
Thickness (t) (mm)	6
Length (mm)	50
Width (mm)	50

Table 3. Geometric characterization of the rivets

Rivet	
Initial height (h_0) (mm)	5, 8, 15
Chamfered angle (α)	30º, 45º, 60º, 90º
Thickness (t_0) (mm)	1.5
Chamfered fillet radius (r_f) (mm)	~0, 0.2

4.2 Case study results and discussion

4.2.1 Joining tests

Initial tests conducted with the set of conditions used to investigate DSSPR in metal sheets did not produce admissible outcomes. The experiments did however produce unexpected results, revealing great amounts of plastic deformation on the rivets, contradicting the conception that the lower mechanical strength of the polymer sheets used would minimize the deformation of the rivet and consequent flaring.

As shown in the figure below, three issues were identified. Figure 11a portraits a recurrent issue, where the rivet would deform in a non-uniform and erratic manner, resulting in a form of irregular collapse of the component. The second issue identified, shown in Figure 11b related to the fact that the expected flaring was not occurring, particularly for lower values of α, and finally the third defect shown in Figure 11c was also identified for smaller values of α, and consisted in a fishhook effect where only the edge of the chamfered angle would suffer plastic deformation preventing flaring from occurring.

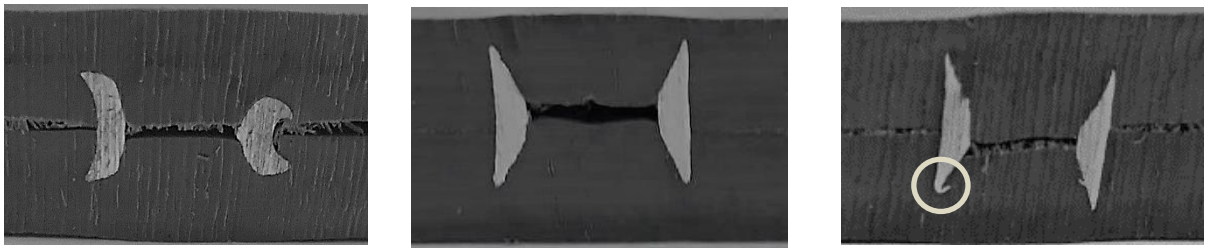

a) b) c)

Figure 11. Failed joining tests: a) Rivet irregularly collapsed; b) Rivet with no flaring; c) Rivet with “fishhook” defect.

After some failed attempts at correcting the first defect, it was conjectured that a potential sliding and relative displacement between the sheets and the rivet was being caused by low friction between the plates and the sheets, affecting the positioning of the rivet and consequently its piercing and flaring trajectory. This effect is intensified by the smaller dimensions of the sheets utilized for producing the test specimens. To assess this hypothesis, the motion of the PVC sheets was restricted, which proved to be effective in eliminating the described defect.

Regarding the second defect, observations allowed to deduce that the sharpness of the chamfered angle was producing a near-straight cut in the sheets, associated to the much higher mechanical strength of the rivet compared to the mechanical strength of the PVC sheets. Alternatively, in cases of extreme sharpness of the rivets chamfered angle, the force level would cause a premature and localized plastic deformation resulting in the fishhook defect depicted in Figure 11c. Accounting for these issues, the small fillet radius r_f feature was introduced, creating a blunt surface on the edge of the chamfered angle that prevented the straight cutting and the fishhook defect from occurring. The benefits of the

introduced feature were backed up by the numerical simulations and experimental testing performed along the following developments, as shown in Figures 12 and 13 respectively.

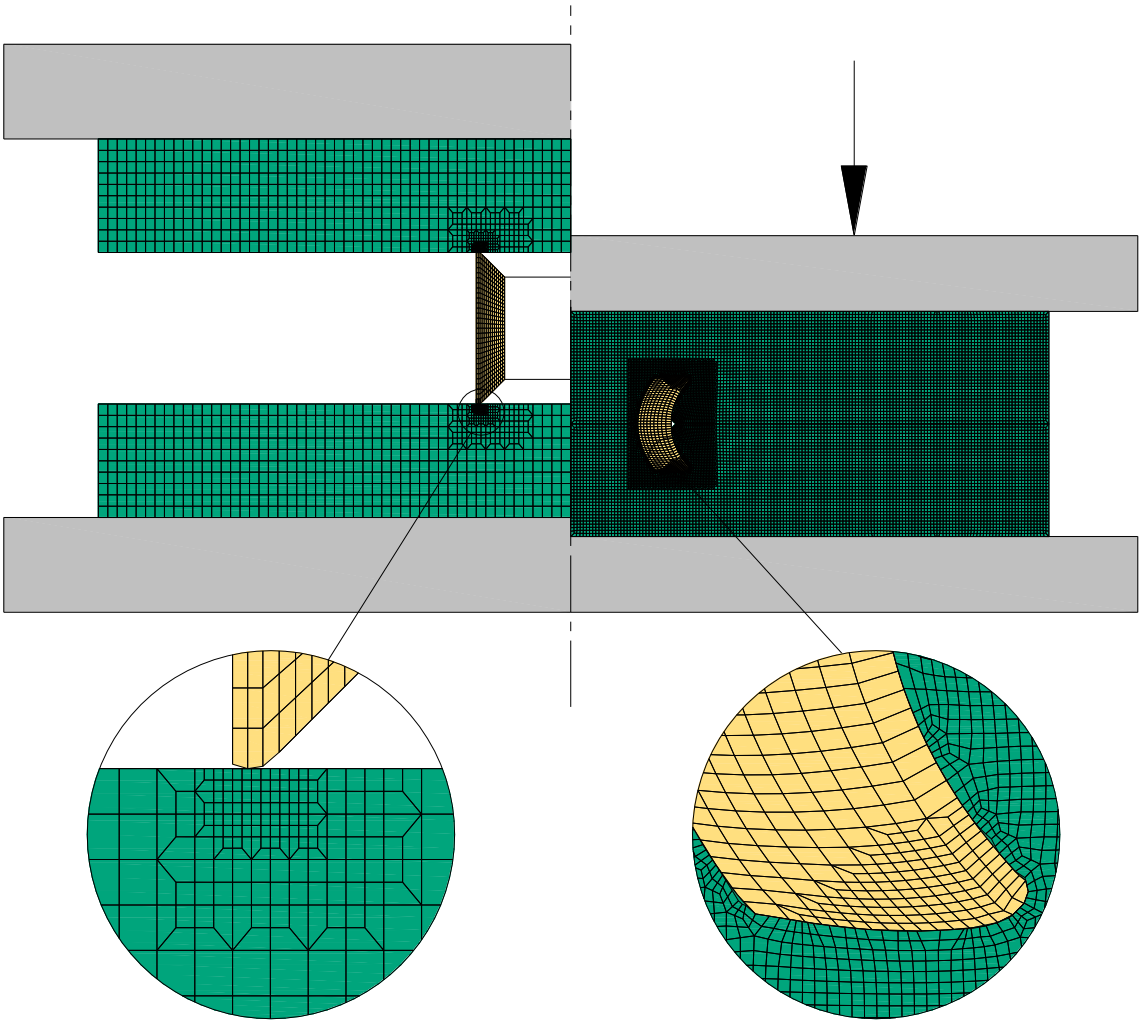

Figure 12. Finite element modelling of double-sided self-pierce riveting of PVC sheets with a stainless-steel rivet at the beginning and end of stroke (h_0= 8 mm and α = 45º). Amplifications show in detail the fillet radius r_f feature.

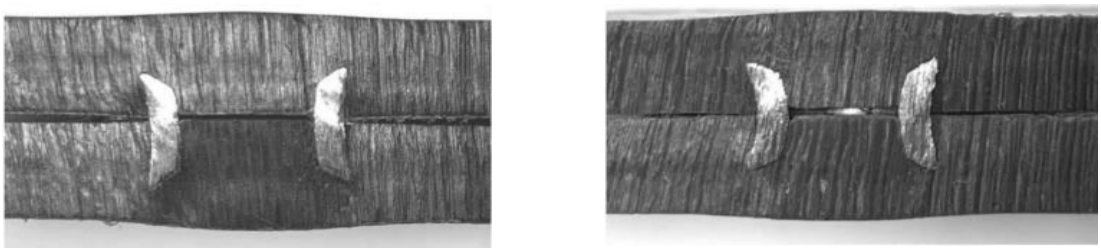

a) b)

Figure 13. Cross-section of two different double-sided self-pierce riveted joints obtained (h_0= 8 mm and α = 45º) with a) sharp chamfered ends $r_f \cong 0$ mm; b) blunt chamfered ends $r_f \cong 0.2$ mm.

Following the successful and consistent implementation of DSSPR in PVC sheets, the tests conducted aimed to evaluate if the chamfered angle α and initial height h_0 of the rivet carried the same influence on the process as previously observed for the aluminum sheets.

Based on the aluminum sheets case study, it was expected that the mechanical interlocking i would increase with the decrease of the chamfered angle α, as the smaller angles promote the outward material flow of the rivet, increasing its curvature. To further back up this statement, an extreme case where a rivet machined with an initial height $h_0 = 8$mm and a chamfered angle α at 90º was compared to a case with $h_0 = 8$mm and α at 30º.

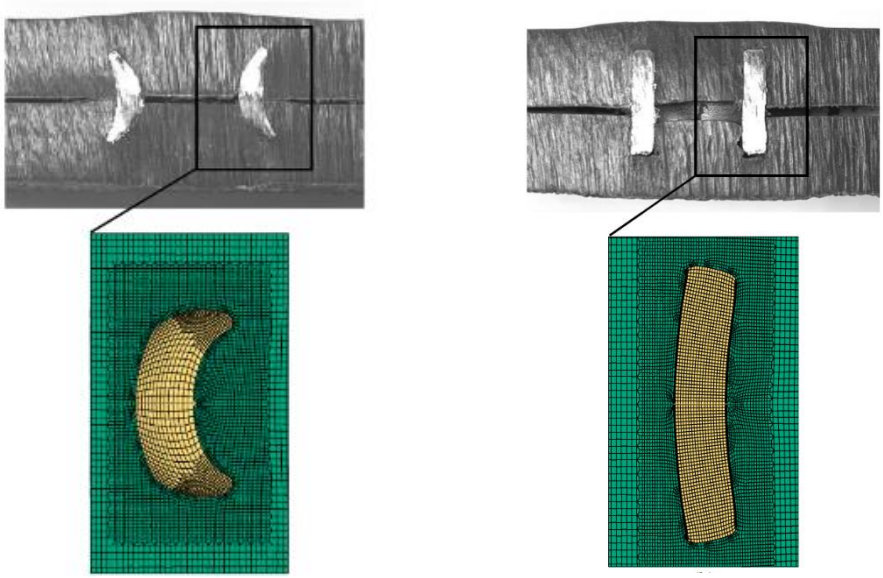

a) b)

Figure 14. Experimental and finite element predicted cross-sections for two different double-sided self-pierce riveted sheets using rivets with an initial height of h_0=8mm, and chamfered angles of a) α = 30º; b) α = 90º

The experimental tests and numerical simulations produced coherent results, confirming that the chamfered angle α consistently influences the amount of flaring produced. As shown, for the case of $\alpha = 90º$, since there was no horizontal force actuating in the chamfered face of rivet, it plastically deformed and slightly tore the surrounding polymeric material, resulting in a strictly vertical penetration, with no interlocking generated. Inversely and as expected, the case where α =30º produced the most interlocking i. This conclusion could therefore be extrapolated to the full range of angles tested, i.e., for a fixed initial height h_0, the interlockings follow the relationship $i(30º) > i(45º) > i(60º) > i(90º)$.

The following figures present the evolution of the riveting force as function of the displacement, comparing data from experimental tests and finite elements simulations. The curves aimed to assess the behavior changes in the riveting force with the angle variations, and to better identify the reliability and precision of the numerical models.

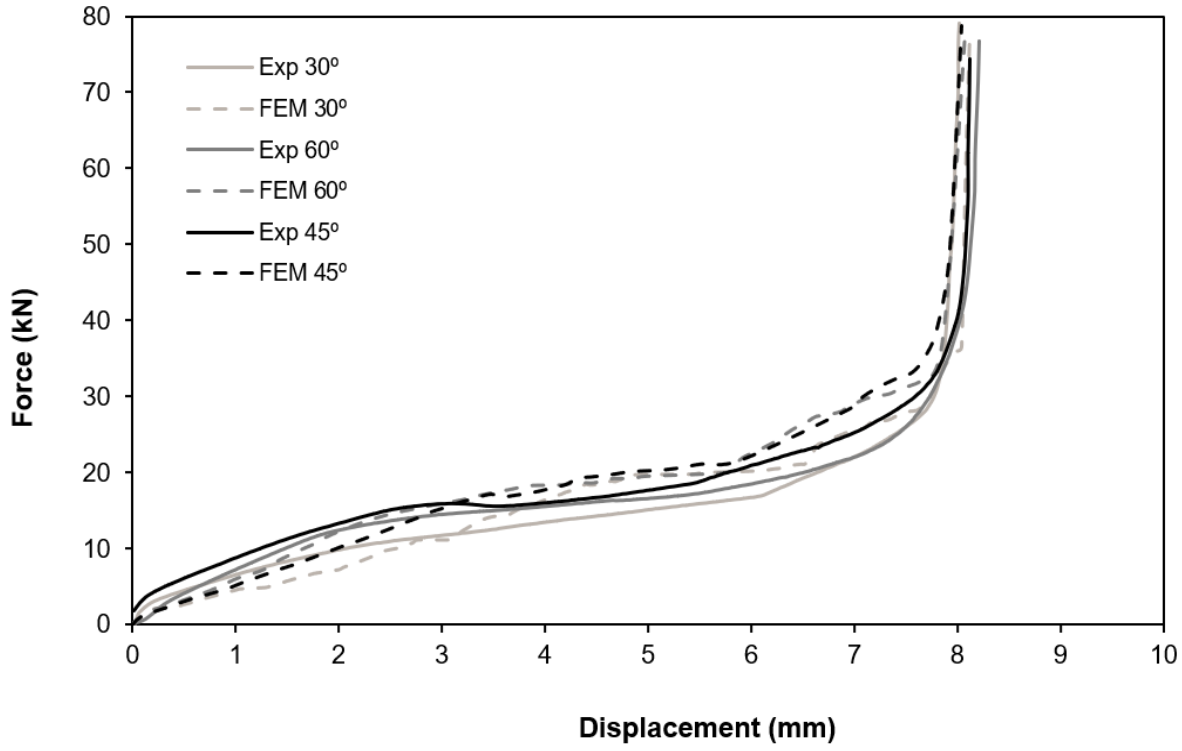

Figure 15. DSSPR of PVC sheets experimental and finite element computed evolutions of the riveting force with stroke using rivets with h_0= 8 mm and: α= 45º, α= 30º and α= 60º

As observed, the finite element simulations predicted the behavior of the riveting force even though slight deviations occurred. These fluctuations were justified by frequent interference and clearance errors in contact interfaces of the materials and by the remeshing operations which often involved manual manipulation of elements to clear those errors, causing loss of information regarding the components' interactions.

The data collected reveals that the maximum compressive force involved in DSSPR of PVC sheets is approximately half than that required in aluminum sheets, but the curve progression is analogous, with the four stages involved in the process being also present [2]. These stages include an initial indentation associated with the contact of the upper and lower sheets with the rivet, a second stage where combined flaring and piercing of the rivet occurs and where the growth rate of the force is slightly lower, followed by a third stage marked by the progressive contact between the upper and lower sheets, and a final stage where the riveting force grows exponentially due to the compression of both overlapped sheets.

It was also worth noting that similarly to what occurred in the aluminum sheets experiments, the rivet with $\alpha = 60º$ required a higher compressive force compared to the rivet with $\alpha = 30º$, although the difference in the PVC sheets between the forces for those cases is not as pronounced. While the process is mainly determined and affected by compressive forces, the occurrence of this slight difference could be explained by fracture mechanics and crack propagation effects of the PVC sheets caused by the sharper chamfered angle of $\alpha = 30º$ in the rivet.

The influence of the initial height h_0 was also analyzed to trace comparative results with those obtained in the case of aluminum sheets [2]. The initial height sensitivity tests were carried with rivets machined

with α =60º as shown in Figure 16. The use of a blunt angle to perform these tests was justified by the need to avoid excessive piercing and tearing of the sheets, as previously concluded.

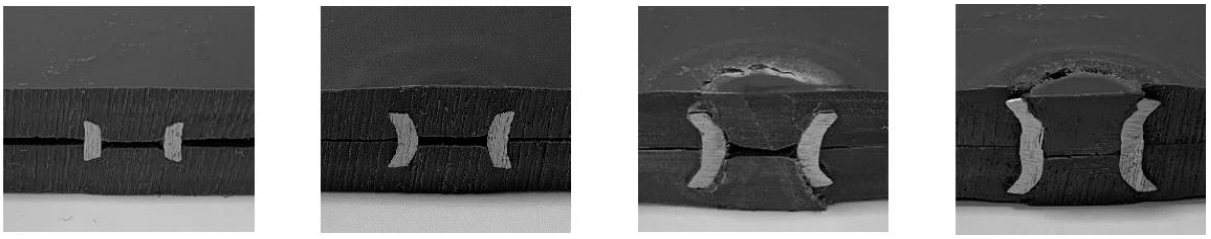

a) b) c) d)

Figure 16. Cross-sections of double-sided self-pierce riveted joints using rivets with α = 60º, and initial heights of a) h_0= 5 mm, b) h_0= 8 mm, c) h_0= 13 mm, d) h_0= 15 mm.

The experimental results once again matched the ones found in metal sheets, as the increase in initial height h_0 caused an increase in the rivet's flaring and interlocking distance. While in the case of $h_0 =$ 5mm barely any flaring occurred, the extreme cases where $h_0 \geq 2t_{sheet}$ saw the maximum amount of flaring and a buckling instability, similarly to what occurred in the aluminum sheets tests [2]. Additionally, given the comparatively lower mechanical strength and strain hardening properties of the PVC sheets, it was observed that a superficial rupture of the material was exposed in these critical cases. Rivets with h_0 within the range of $h_0 \leq 2t_{sheet}$ created admissible joints, and as results indicated, better interlocking was incrementally achieved with the increase of h_0 until its critical instability height value ($h_0 \cong 2t_{sheet}$) was reached.

4.2.2 Destructive tests

The experimental work of DSSPR in polymer sheets was concluded by performing a destructive test to assess the joint's performance under shear and peel stresses. The specimen selected included a rivet with α =45º and h_0 = 8mm. The PVC sheets had a length of 100 mm and a width of 50 mm, and the specimens used in the peel test underwent a bending procedure at 90º in their middle point (Figure 17). The behavior of the solicited load as function of the displacement is shown in Figure 18 for both shear and peel tests.

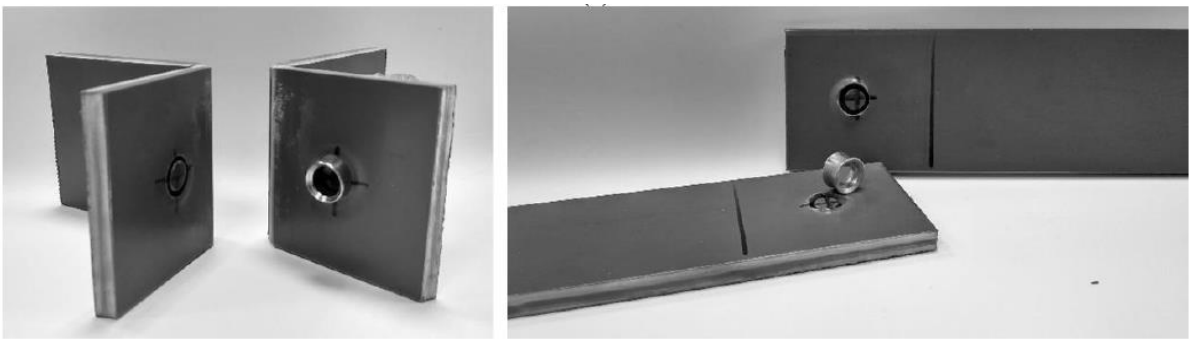

Figure 17. Photographs of the peel (left) and shear (right) specimens after being tested.

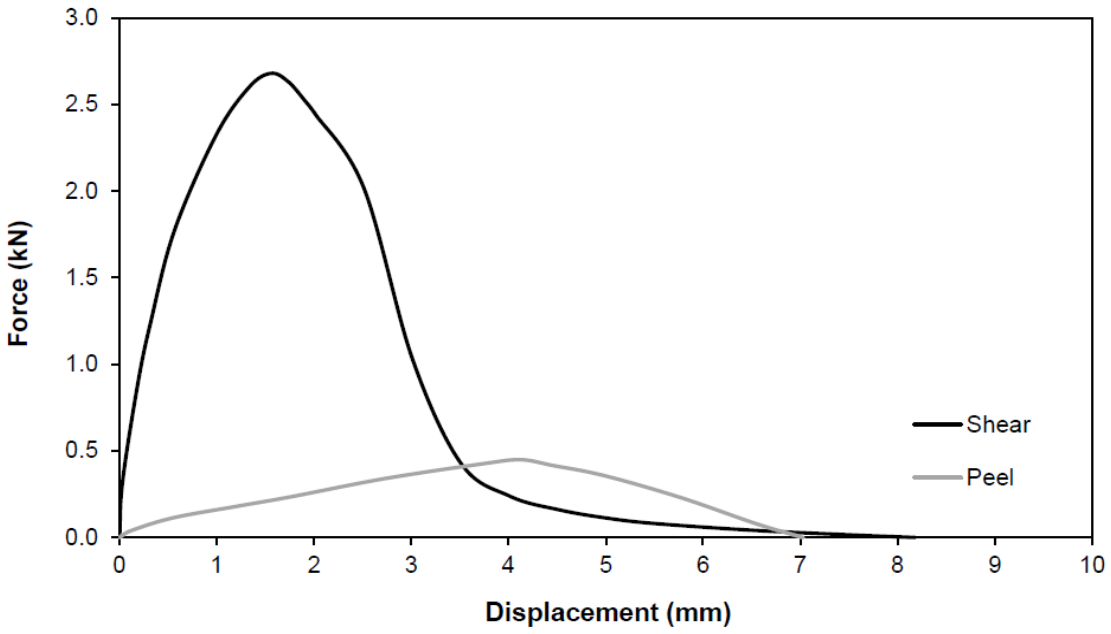

Figure 18. Experimental evolution of the force with displacement of destructive peel and shear tests of a DSSPR joint using a rivet with h_0= 8 mm and α= 45º

As Figure 18 shows, the joint achieved approximately 2.7 kN of shear force before reaching a critical failure, and a pull-out force of around 500 N. The poorer performance of the DSSPR joint compared to the aluminum sheets case was expected given that failure starts to develop in the sheets and the

mechanical strength of the PVC sheets is lower. The ratio between the critical loads achieved was however observed to be of the same order of magnitude than the one obtained in the aluminum sheets. These destructive tests allowed to observe a completely distinctive behavior in the deformation mechanics associated with the solicited stresses, justifying the comparatively lower critical values achieved. In the shear tests of the aluminum sheets, as the load increased, the strain hardening of the materials delayed severe plastic deformations from occurring until the material with lowest mechanical strength (i.e., the aluminum) sustained a critical failure. In the case of the PVC sheets, due to the higher elasticity of the polymer, the critical failure was caused by the sudden detachment of the rivet from one of the sheets.

This same detachment of the rivet was equally observed in the pull-out tests, while in the case of the aluminum sheets, the critical failure was caused by the tear of the sheet in the area surrounding the flared rivet.

Once more, this case study presented supported the potential of the DSSPR technology, expanding its range of applications in terms of material selection. It was also possible to identify key limitations to eventual functions, as the mechanical properties of polymeric materials could completely preclude the application of DSSPR given their inherent elastic and plastic behavior. Regardless, the experimental work indicated that the application of DSSPR to polymers was feasible taking into consideration the correct selection of geometric parameters.

5. DSSPR of dissimilar materials

The series of experimental testing and results gathered from the application of DSSPR for sheets made from the same material motivated the interest of expanding knowledge about the joining technology regarding what was considered to be one of its strongest features when compared to conventional solutions currently available: the ability to mechanically join dissimilar materials [15]. Self-pierce riveting, as one of the most common joining by forming technologies used in dissimilar materials, suffers from limiting factors inherent to its process and deformation mechanics. The limitation of the sheet's thicknesses, the range of materials, and the need to prioritize the positioning of the sheets depending on material properties heavily restrict the application of SPR specifically in dissimilar materials.
The following work aimed therefore to assess the performance of DSSPR under conditions that seemed to set the application limit under which the analogous process of SPR could operate, by testing the technology in materials with very different mechanical properties and relatively thick sheets.

5.1 Testing parameters description

Previous experimental work focused on accessing the applicability of DSSPR and how the geometric parameters of the rivet influenced the produced outcome. With that fairly precise conception regarding the behavior of the riveting process in both PVC and aluminum, the tests carried out in this section aimed to observe the influence and interaction between the dissimilar materials in the resulting joint. The geometric parameter selection, based on that premise, is presented in the tables below.

Table 4. Geometric characterization of PVC and aluminum sheets

PVC and Aluminum Sheets	
Thickness (t) (mm)	5
Length (mm)	50
Width (mm)	50

Table 5. Geometric characterization of rivets

Rivet	
Initial height (h_0) (mm)	8
Chamfered angle (α)	30º, 45º, 60º
Thickness (t_0) (mm)	1.5
Chamfered fillet radius (r_f) (mm)	~0, 0.2

Experimental and numerical work developed in this case study were comprised of two different phases. The first phase, similarly to the previously presented case study, consisted of verifying and validating

the implementation of DSSPR in dissimilar materials while analyzing potential performance or process vulnerabilities. The consequent phase emerged from the results and observations gathered and aimed to introduce major optimizations and adaptations to the process.

5.2 Case study results and discussion

5.2.1 Joining tests

Given the reliability in results of previous numerical simulations, the joining tests planned for this work were selected after extensive analyses of finite element simulations. The initial simulations followed the structure of previous studies, assessing the performance of DSSPR with different validated chamfered angles α. The first cases numerically modeled, as shown in Figures 19 and 20, included the typical rivets used so far with angle α of 30º,60º and 45º.

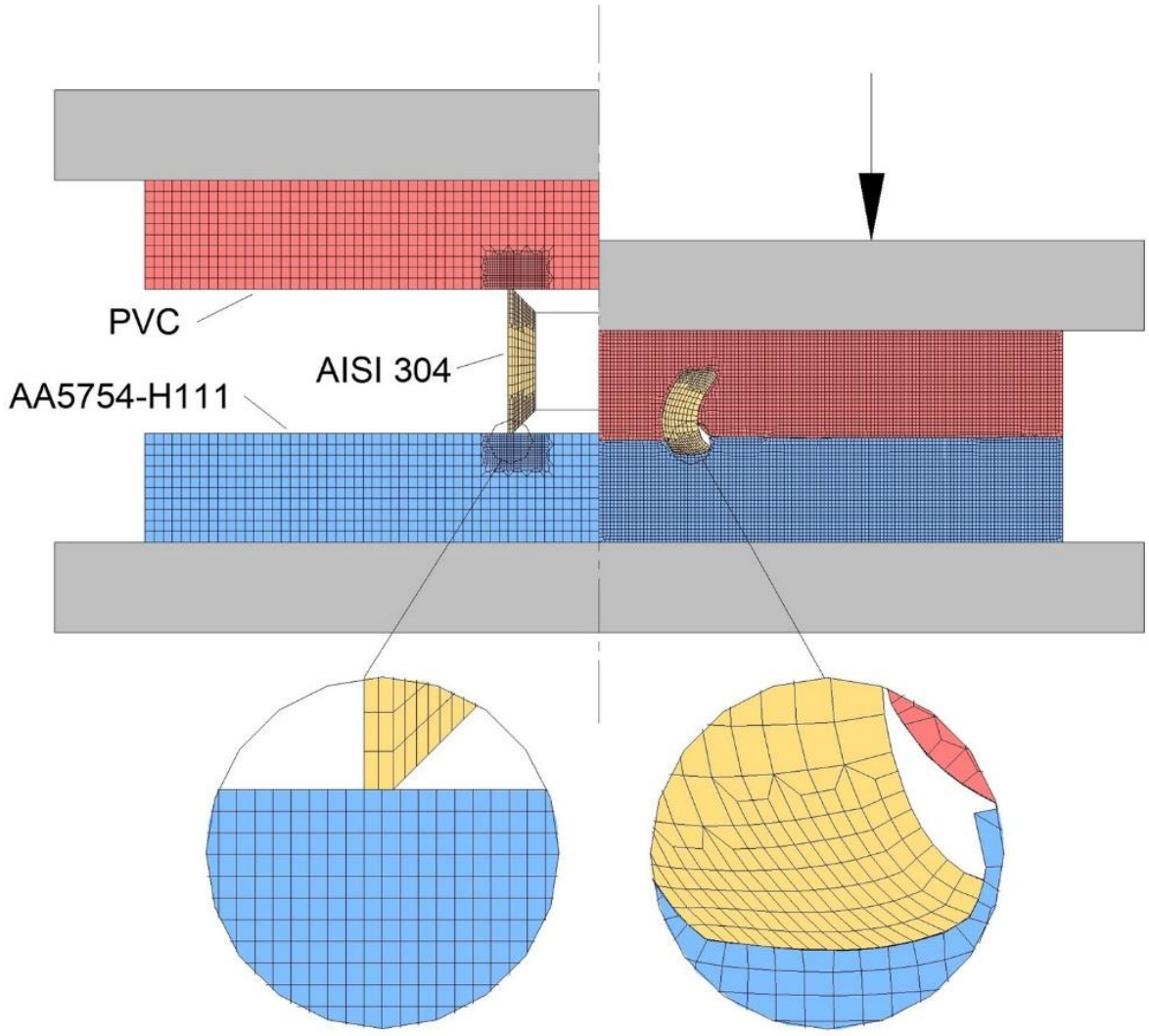

Figure 19. Finite element model of double-sided self-pierce riveting of AA5754-H111 aluminum and PVC sheets with AISI 304 stainless-steel rivets with h_0= 8 mm and α= 45º at the beginning (left side) and end of the process (right side)

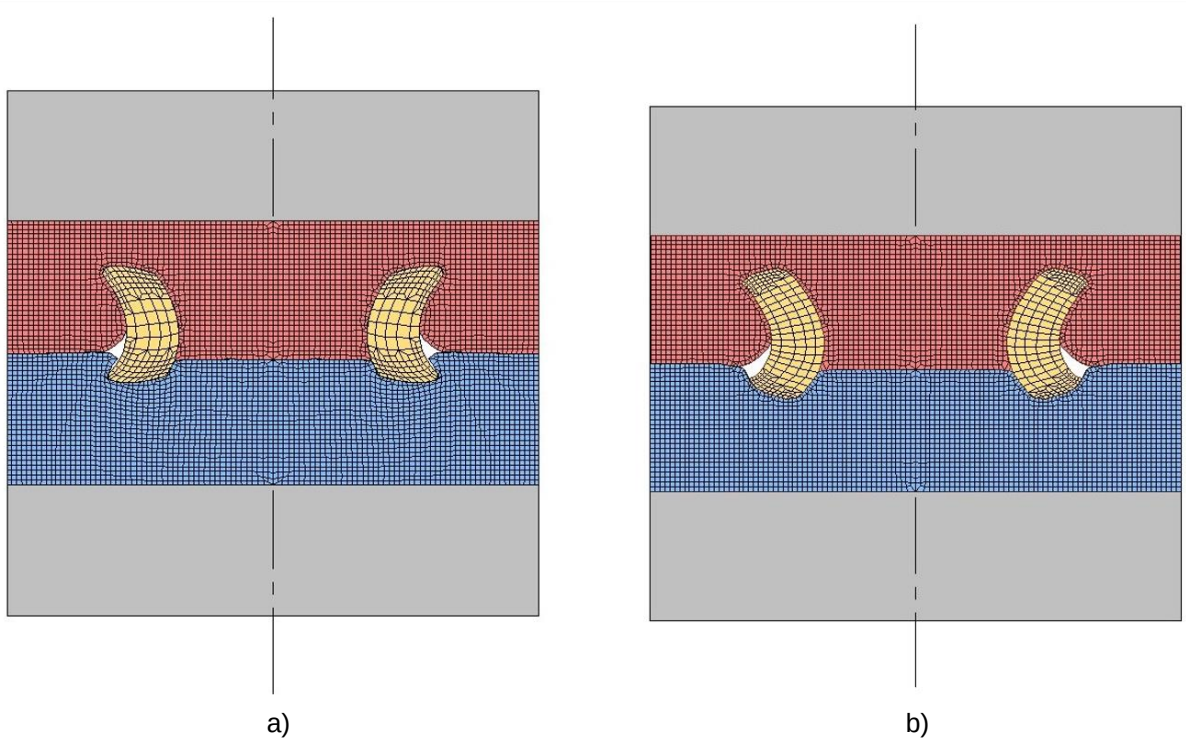

Figure 20. Finite element predicted cross-sections of DSSPR to the connection of AA5754-H111 aluminum and PVC sheets with AISI 304 stainless-steel rivets with h_0= 8, and a) α= 30º b) α= 60º

Numerical results observed seemed to indicate that clamping would in fact occur, particularly in the case where α equaled 30º, which aligned to the observations drawn out formerly. However, it was verified in all cases that the aluminum sheet was not suffering significant piercing action of the rivet, although the rivet was flaring. This effect particularly revealed the complexity involved in the interaction between the materials. Furthermore, the asymmetric penetration distance between the materials in all cases was also considered a relevant, yet expected effect caused by the discrepancy in the material's mechanical strengths.

With these sets of results in consideration, a new variation of the geometric properties of the rivet was modeled in an attempt to increase joint symmetry and achieve better piercing of the aluminum sheet. The concept for the use of different angles in the rivet was consequently simulated. As shown in the left detail of Figure 21, the angle α_{Al} (positioned on the aluminum sheet) and the angle α_{PVC} (positioned on the PVC sheet) were assigned with the values of 30º and 60º, respectively. The expected outcome of this configuration was centered around the observed influences of the chamfered angle on each material. The use of α_{Al}= 30º would favor the penetration of the rivet in the aluminum sheet, which was desirable, while for the PVC sheet, a mitigation of the piercing effect would presumably promote a symmetric deformation of the rivet while avoiding potential tearing of the sheet. For that reason, the angle α_{PVC} at 60º was assigned since its bluntness would carry the intended function.

The resulting numerical simulation of this rivet configuration (Figure 21) resulted in a potential improvement in the penetration depth of the aluminum sheet, but no improvements on the rivet's symmetry was observed. Figure 21 shows in detail the initial shape of the rivet and the joint obtained, after elastic recovery.

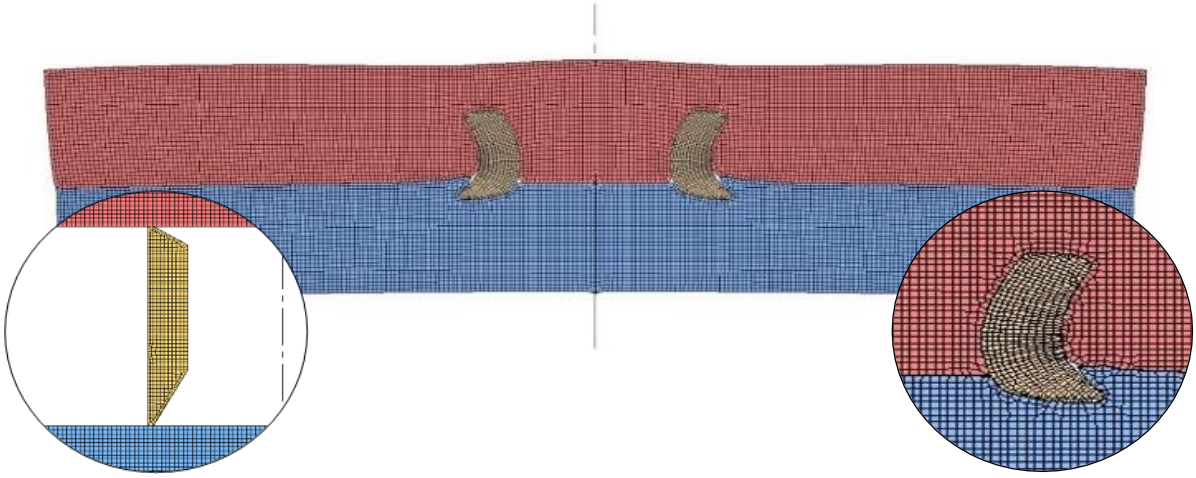

Figure 21. Finite element model of double-sided self-pierce riveting of AA5754-H111 aluminum and PVC sheets with AISI 304 stainless-steel chamfered angle rivet with two-angle configuration (α_{Al}= 30º, α_{PVC}= 60º) after elastic recovery. Left detail shows the initial step of the simulation and right detail shows a zoom-in of the final step.

With the evidence provided by the simulations, experimental work of the conditions evaluated was performed. The visual condition of the joints obtained are shown below in Figure 22. Despite of some differences, the numerical simulations accurately predicted the asymmetric piercing associated with conventional rivets.

For the case of α= 30º, excessive penetration occurred as a result of small deviations in the rivet chamfered angle and shape, resulting in a superficial tear of the PVC sheet suggesting the existence of susceptibility to fracture associated with high levels of piercing of the PVC sheet. The resulting piercing of the aluminum sheet was also superficial implying poor interlocking to the sheet, which was also predicted.

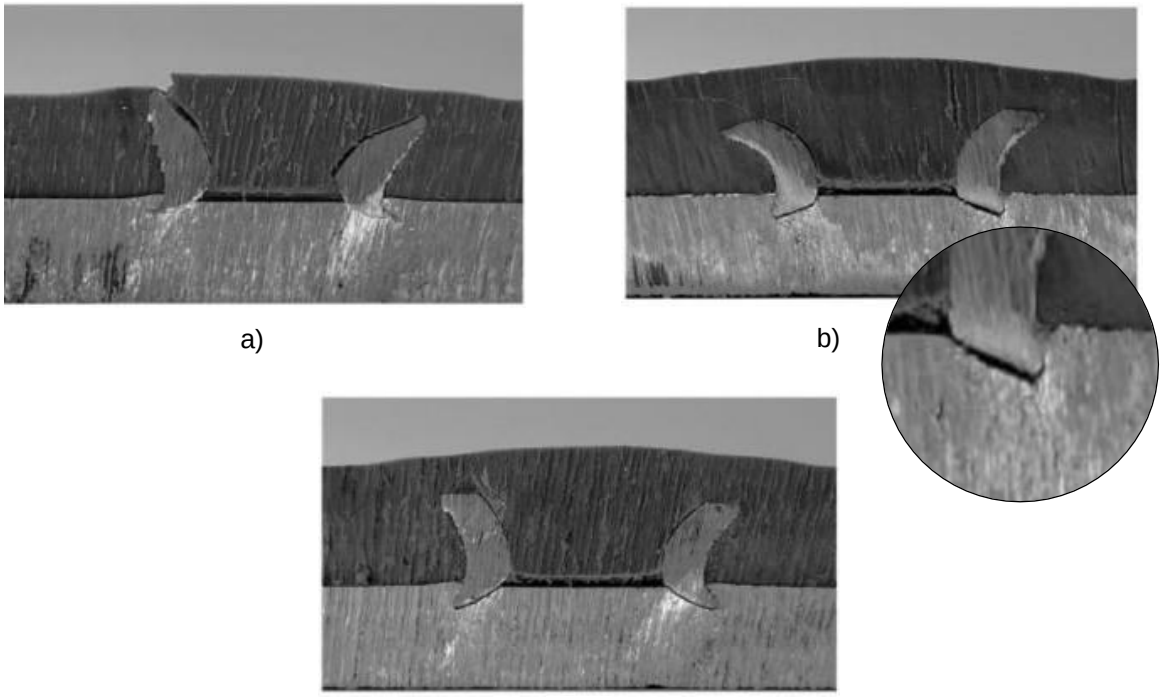

Figure 22. Experimental cross-sections for the test cases corresponding to values of the chamfered angles a) α= 30º b) α= 60º c) α_{Al}= 30º, α_{PVC}= 60º

From observations made on the rivet with two different angles in its ends, a better interlocking caused by the sharper angle α_{Al} on the aluminum sheet occurred, while the blunt angle α_{PVC} prevented excessive piercing of the PVC sheet. The outcome still did not deliver satisfactory results, as symmetry in penetration depth was not achieved, and a significant protrusion was formed in the PVC sheet as a result of material displacement caused by the rivet. These protrusions observed in the cross-sectioned tests were however amplified by the excessive elastic recuperation of the joint caused by the cross-sectional cut of the specimens, which eliminated the circumferential constraint imposed by the materials. The numerical simulation prediction (Figure 21) included the elastic recuperation behavior of the materials and allowed a more accurate visualization of the size of the original protrusion.

Furthermore, from an industrial implementation perspective, the two-angle rivet would imply additional costs to the process, as the pre-positioning of the rivet would have to account for the angle orientation in relation to each sheet, causing an increase of the overall cycle-time of the process and the risk of producing defected joints due to a mismatch between the assigned angles of the rivet for each sheet.

In terms of the evolution of the riveting force, observations were made once again to the different stages associated with the process. In particular, and as depicted in Figure 23, it was noticed a region starting in ‘A’ in which the force progressively increased with the compression of the rivet up to the point of contact between both sheets, and where the contact between the compression tool and the upper PVC sheet is limited to the area directly above the rivet. From this moment to the point marked by ‘B’, a slight change in the riveting force was associated with the increasingly larger contact area between both

sheets and between the upper die and the PVC sheet, followed by a steep increase in force caused by the full contact of the interacting components.

The same evolution of the riveting force with stroke was also analyzed for the remaining rivet configurations, as presented in Figure 24.

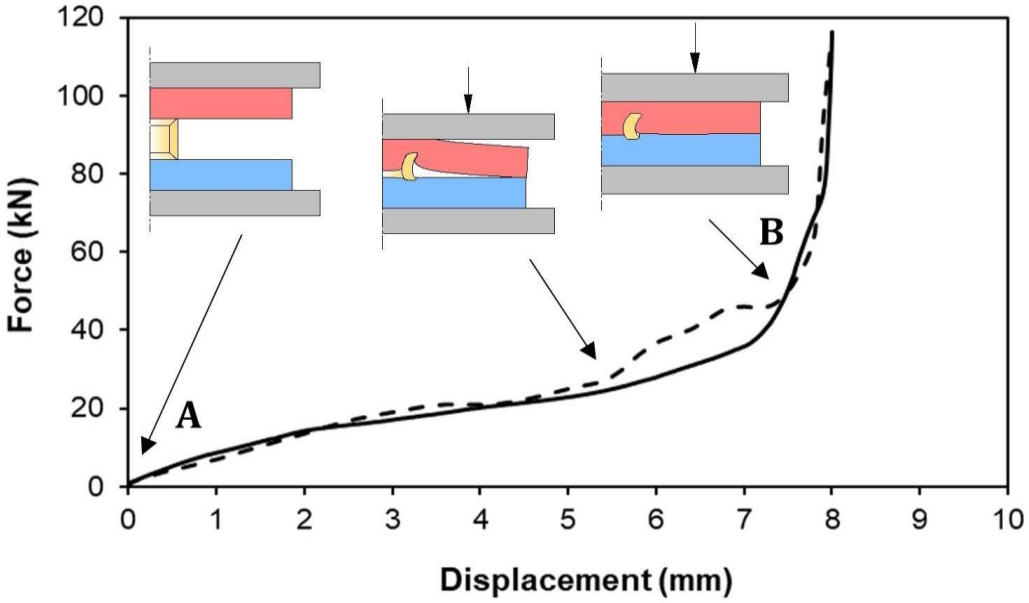

Figure 23. Experimental and finite element computed evolutions of the riveting force with stroke using rivets with h_0= 8 mm and α= 45º

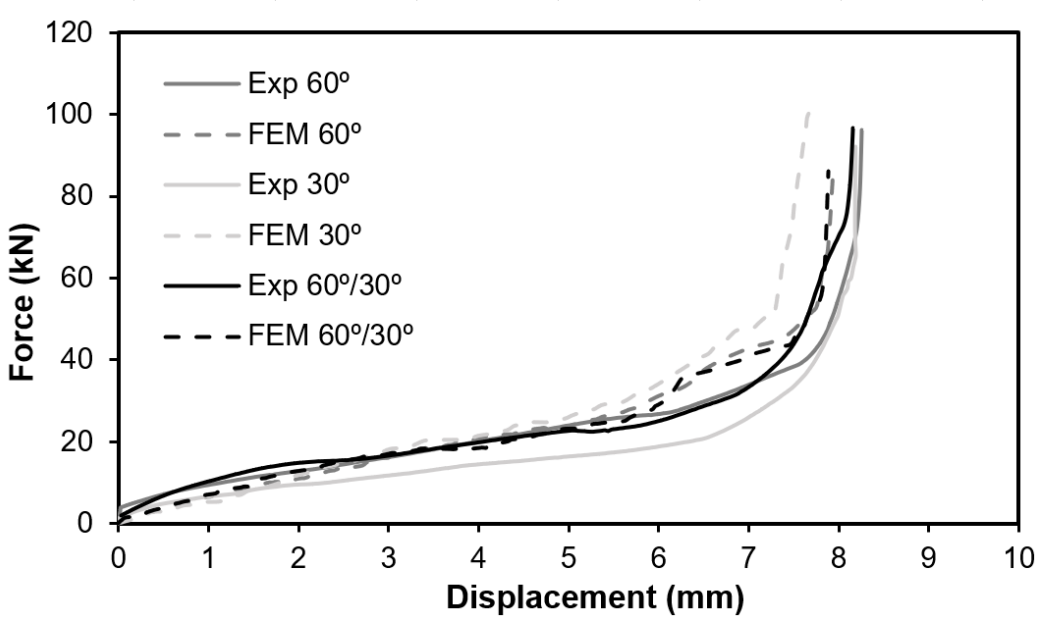

Figure 24. Experimental and finite element computed evolutions of the riveting force with stroke using rivets with h_0= 8 mm and chamfered angles with: α= 30º, α= 60º and α_{Al}= 30º, α_{PVC}= 60º

Results from all tests carried demonstrated a similar behavior of the curve, with the maximum riveting force averaging at 60 kN, equally obtained for the case of similar metal sheets, and nearly twice as much compared to the maximum average value obtained in the similar polymer sheets tests of 30 kN.

Following the unsatisfactory results, further optimization and manipulation of the process was required. This necessity was matched with the interest of developing solutions that could simultaneously improve DSSPR from an industrial implementation standpoint. The next phase of the study consisted precisely in studying a manipulation of the process that could improve the rivet's piercing symmetry, by separating it in two strokes. Subsequently, a second alternative maintaining a single stroke is presented and discussed.

6. DSSPR of dissimilar materials: Process variants

As portrayed in the previous chapter, the concept of double-sided self-pierce riveting applied to relatively thick sheets of dissimilar materials demonstrated its potential, but at this stage, still lacked valid and meaningful results in terms of symmetry and joint invisibility achieved due to the complex interaction of materials. Additionally, the introduction and testing of the two-angle rivets fueled the interest in further exploring options for optimizing the process in general, while simultaneously considering its industrial implementation, viability, and flexibility.
This chapter was therefore compartmentalized in two subsections introducing two variation options for the process.

6.1 Double-stroke DSSPR

The first studied variant consisted in separating the process in two strokes, forcing the rivet firstly through the sheet with highest mechanical strength and subsequently through the sheet with the lowest mechanical strength in a separate compressive phase [15]. For the first stage, a dedicated tool consisting of a conical punch and a bolster, depicted below in Figure 25, was used to compress half of the rivet through the aluminum sheet while maintaining the geometric integrity of the opposite chamfered angle. The second stage of the process consisted in the removal of the tool and the positioning of the PVC sheet above the undeformed side of the rivet and respective compression of the sheets to create the desired mechanical interlocking.

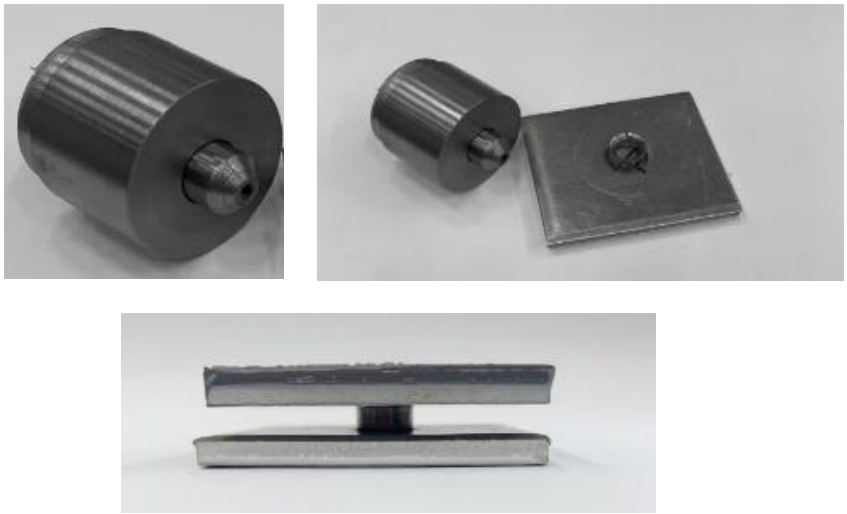

Figure 25. Photographs of punch and die used (top), aluminum sheet after first stroke (top right) and PVC sheet setup at the beginning of the second stroke (bottom) of the proposed DSSPR variation.

The following figure presents the finite element model of the experimental test described above, depicting the geometric evolution of the riveting with each stroke, where the intermediary step represents simultaneously the end of the first stroke and the beginning of the second stroke. As shown, promising

results were expected from the new two-stroke DSSPR, as it appeared to solve both the horizontal and vertical asymmetries existing in the conventional DSSPR application in dissimilar materials.

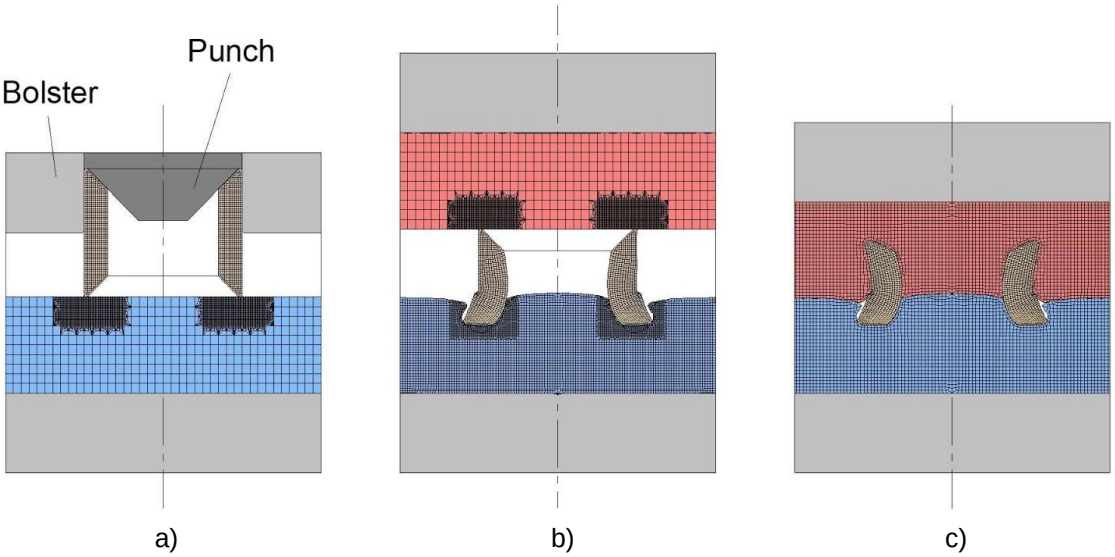

Figure 26. Finite element model of proposed two-stroke DSSPR: a) Beginning of first stroke; b) Beginning of second stroke; c) Ending of second stroke.

The design and geometry of the dedicated tool proved to have a determining impact on the structural integrity of the rivet and ultimately on the quality of the joint, as multiple iterations for the tool's geometry were developed and simulated before reaching the presented variant in Figures 25 and 26. In Figure 27, different iterations for the tool and their simulated outcomes are presented.

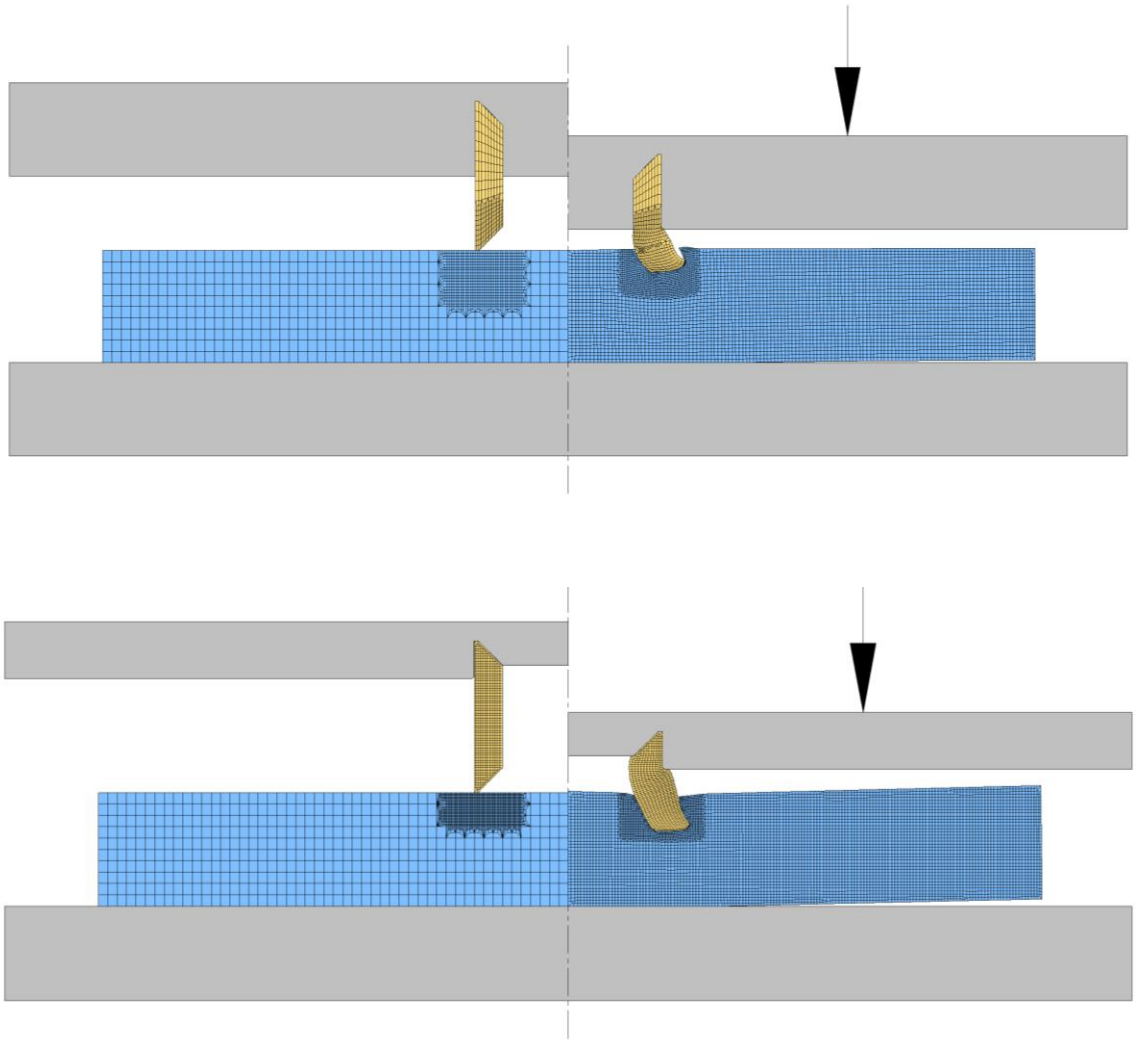

Figure 27. DSSPR double-stroke finite element simulations at the beginning (left side) and end of the process (right side) of failed punch and die geometric variations.

The iterations presented above on Figure 27 allowed to conclude that the tool would have to provide enough freedom for the rivet to increase in thickness, and a free rivet height that would promote half of it to pierce through the aluminum sheet. As shown, the top figure shows a severe deformation of the rivet caused by its increase in thickness due to excessive constraining by the tool, while the bottom figure shows a severely deformed rivet caused, however, by its increase in thickness due to excessive free rivet height. The variant in Figure 26 yielded the best results both in terms of the rivet's piercing and deformation and was therefore the adopted solution for the following set of experimental and destructive tests.

The experimental tests were performed using the rivets with the same chamfered angles in both sides, as well with the same geometric variables as for the initial tests that were carried out for dissimilar materials. These tests aimed to validate and verify the sensitivity of the joint to the variation of the chamfered angles.

a) b) c)

Figure 28. Experimental cross-sections of double-stroke DSSPR in dissimilar materials using rivets with h_0= 8 mm and: a) α= 30º b) α= 45º c) α= 60º

The results allowed to conclude that the proposed variant of using a double-stroke compressive process did in fact improve the rivet's symmetry both horizontally and vertically. Upon visual inspection, the protrusion of the PVC sheet was also reduced when compared to the initial iterations, since lesser material displacement occurred in the PVC sheet due to the improved piercing of the rivet in the aluminum.

Furthermore, the value of the interference (i) for the case where α=45º was measured at 0.92mm, a value similar to the interference obtained in similar material joints of aluminum sheets [2], suggesting that the dissimilar material connection was successfully achieved.

The experimental and numerically modeled curves of riveting forces with displacement for the experimental case where α=45º are provided in Figure 29, presenting both the evolution for the first stroke by action of the tool and punch (black curves starting in 'I') and for the second stroke where the PVC sheet is compressed against the already riveted sheet (grey curves starting in 'II' and ending in 'III').

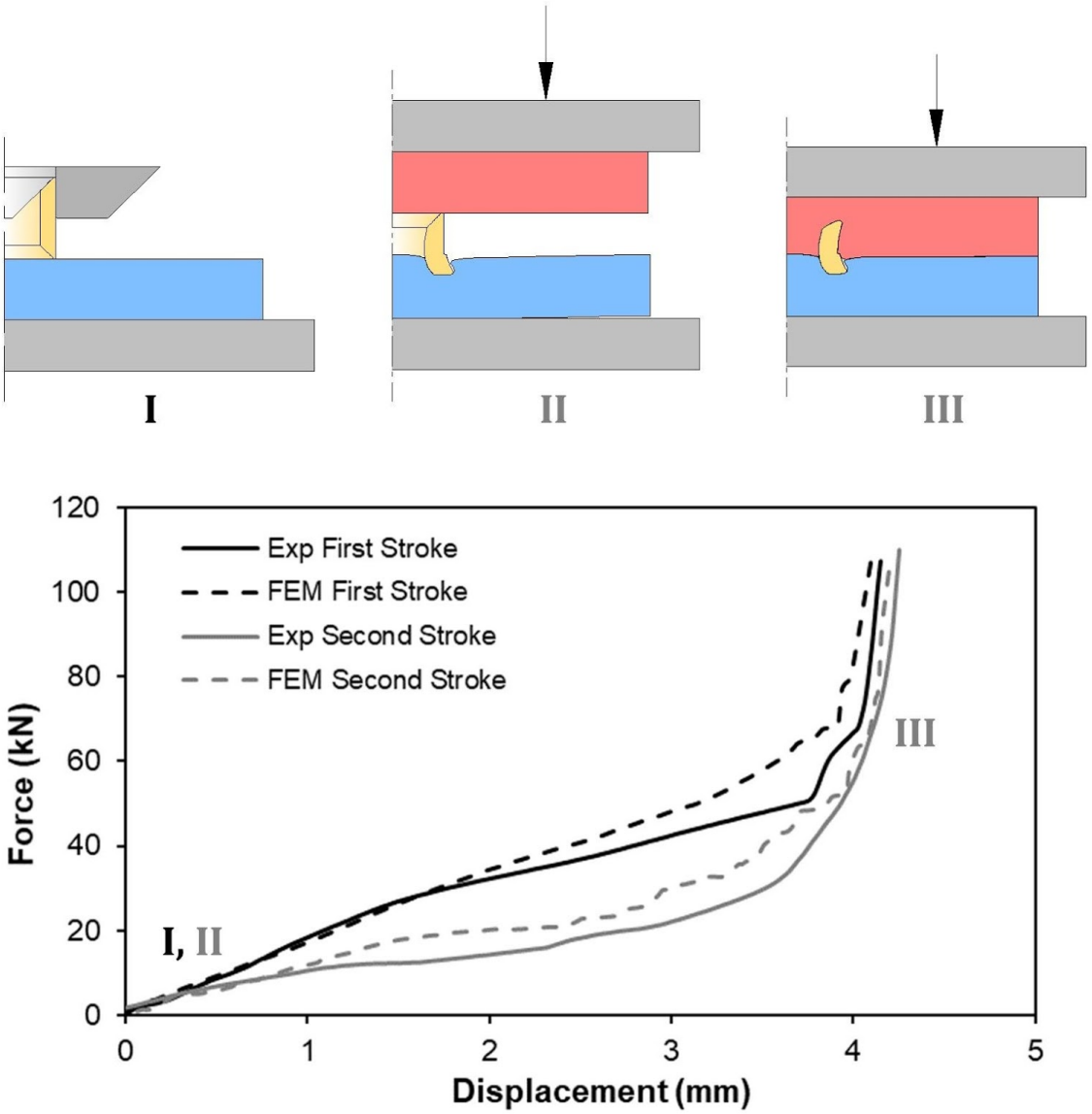

Figure 29. Experimental and finite element predicted evolution of the riveting force with displacement for the double-stroke double-sided self-pierce riveting of AA5754-H111 aluminum and PVC sheets with AISI 304 stainless-steel rivets with h_0= 8 mm and chamfered angles α= 45º

6.2 DSSPR complemented with flat-bottom holes

In recent developments, one other variant solution was proposed and experimented [16]. The implementation of this variant served the main purpose of correcting the asymmetry and protrusion issues involved in DSSPR of dissimilar materials. Additionally, the concept also aimed to introduce a feature that would benefit the joining process from an industrial implementation perspective by providing a positioning feature for the rivet, as later discussed.

The concept consisted of a pre-operation of machining or shaping of a circular flat-bottom hole with diameter of approximately the rivet's outer diameter in the highest mechanical strength sheet, in this case being the aluminum sheet. Conceptually, the slot would benefit both vertical and horizontal symmetries by facilitating the rivet's piercing in the aluminum sheet and reducing the amount of piercing the PVC sheet would be subjected due to a reduction in the free rivet height.

Finite element simulations were carried out to analyze the effects of the slot according to its geometry, more specifically its depth, as the following Figures 30 and 31 show.

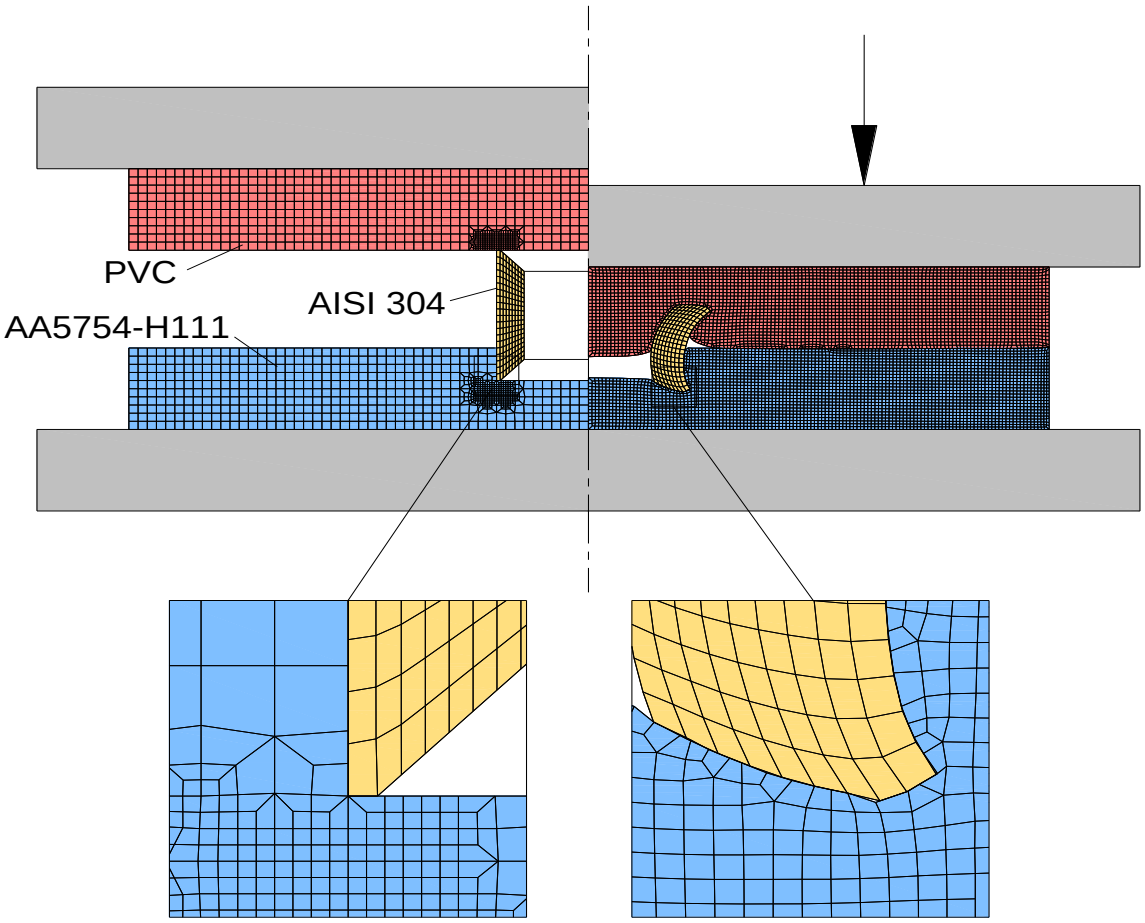

Figure 30. Finite element model of DSSPR with flat-bottom holes on AA5754-H111 aluminum sheets and its connection with PVC sheets through AISI 304 stainless-steel rivets with h_0= 8 mm and chamfered angles α= 45º at the beginning (left side) and end of the process (right side).

In the initial numerical simulations, observations were made regarding changes in material flow in the interacting components, and in the deformation mechanics involved.

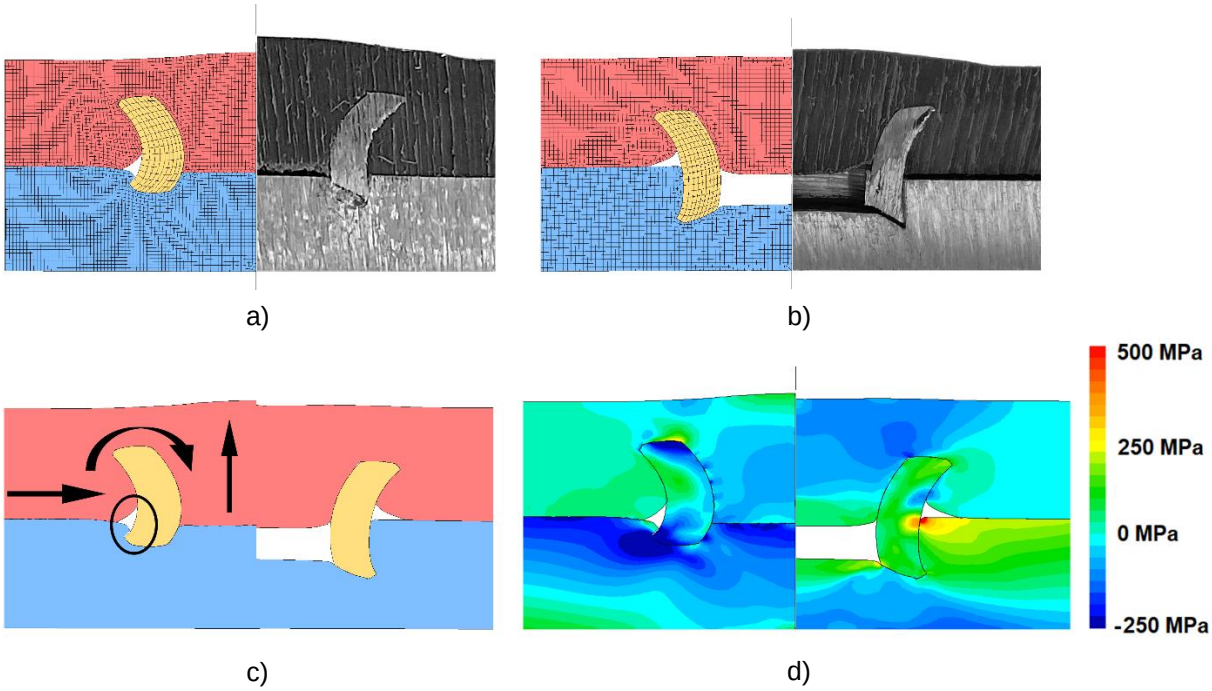

Figure 31. Double-sided self-pierce riveting (DSSPR) of AA5754-H111 aluminum and PVC sheets with AISI 304 stainless-steel rivets with chamfered angles of 45º.
a) Finite element predicted geometry and photograph of experimental cross for conventional DSSPR.
b) Finite element predicted geometry and photograph of the cross section after elastic recovery for DSSPR with 2mm depth flat-bottom-hole.
c) Finite element predicted geometry comparison between cases (a) and (b).
d) Finite element distribution of radial stress (MPa) after elastic recovery for conventional DSSPR (left) and DSSPR with flat-bottom hole (right).

As observed by comparing Figure 31a and 31b, the flat-bottom hole affected the material displacement of the PVC sheets, suggesting a potential improvement in the amount of protrusion formed due to a better filling of the empty volume existing between sheets. A visible overall improvement in the joint's symmetry was also observed, hinting at the validation of initial concept predictions. A direct comparison between both simulations is also presented in Figure 31c.

In Figure 31d, the finite element predicted distributions of the residual normal stresses for the conventional and the optimized version of DSSPR were quantified. As shown in the proposed version of DSSPR, compressive stress values are distributed along the lower contact interface between the rivet and the flat-bottom hole. These stresses were expected to positively influence the constraint between both sheets, obstructing tangential or vertical movement due to the friction generated between the rivet and the aluminum sheet. This effect suggested that the joining of the rivet to the aluminum sheet is caused by a force-closed mechanism associated with the residual stresses at that region. However, no relevant interlocking occurred, suggesting the absence of the form-closed mechanism observed in conventional DSSPR. Based on this initial approach and observations acquired, an assessment of the sensitivity of the joint to the depth of the slot was performed, as portrayed in Figure 32.

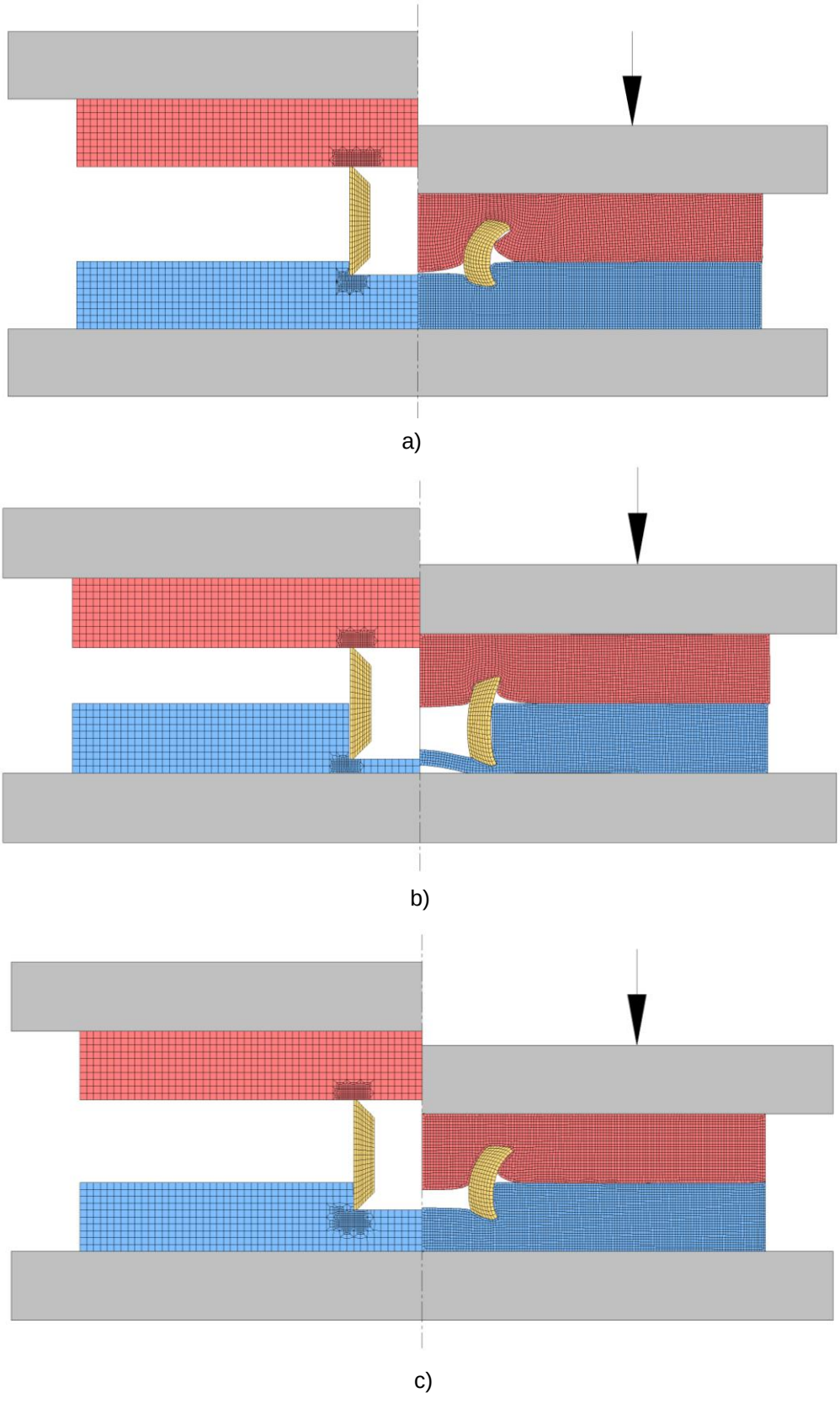

Figure 32. Finite element models of DSSPR in dissimilar materials with flat-bottom holes with a) 1mm depth; b) 4mm depth; c) 2mm depth

Experimental tests were performed to verify the simulations' results pertaining the process' sensitivity to the slot's depth (d_p). Figure 33 presents the experimental resulting joints with rivets with a constant initial chamfered angle of α=45º. These results matched the predicted behaviors of the joint, where the slot with 2mm depth provided the better symmetry between the rivet and aluminum sheet. Increasing the hole's depth also affected positively the size of the protuberance created in the PVC sheet by reducing it vertically. This reduction was associated with the empty space within the rivet provided by the slot, which allowed material from the PVC sheet to flow towards the empty gap. However, a limitation was also identified in the sheet's geometry to the application of this variant. In the case of the deepest slot, a critical failure occurred in the aluminum sheet, suggesting that the use of this feature should be limited to sheets with enough thickness to sustain the deformation and stresses introduced without failure. In that sense, it was considered that this application was limited to the use in sheets of at least 3mm thickness, considering an appropriate slot depth.

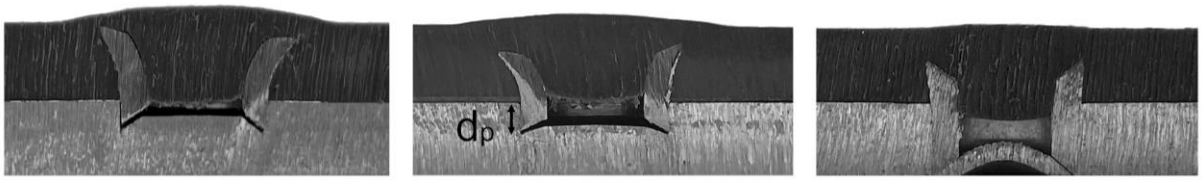

a) b) c)

Figure 33. Experimental cross-sections of DSSPR in dissimilar materials with flat-bottom holes with a) 1mm depth b) 2mm depth c) 4mm depth

While a proper definition of the slot's depth and sensitivity was identified, no relevant influence or impact was drawn from the implementation and depth variation of flat-bottom holes in terms of the interlocking achieved in the joint. In that sense and given the already well-established influence of the rivet's chamfered angles in the interlocking between sheets, finite element simulations and experimental tests in specimens with flat-bottom holes were carried out to assess the joint's sensitivity to chamfered angles.

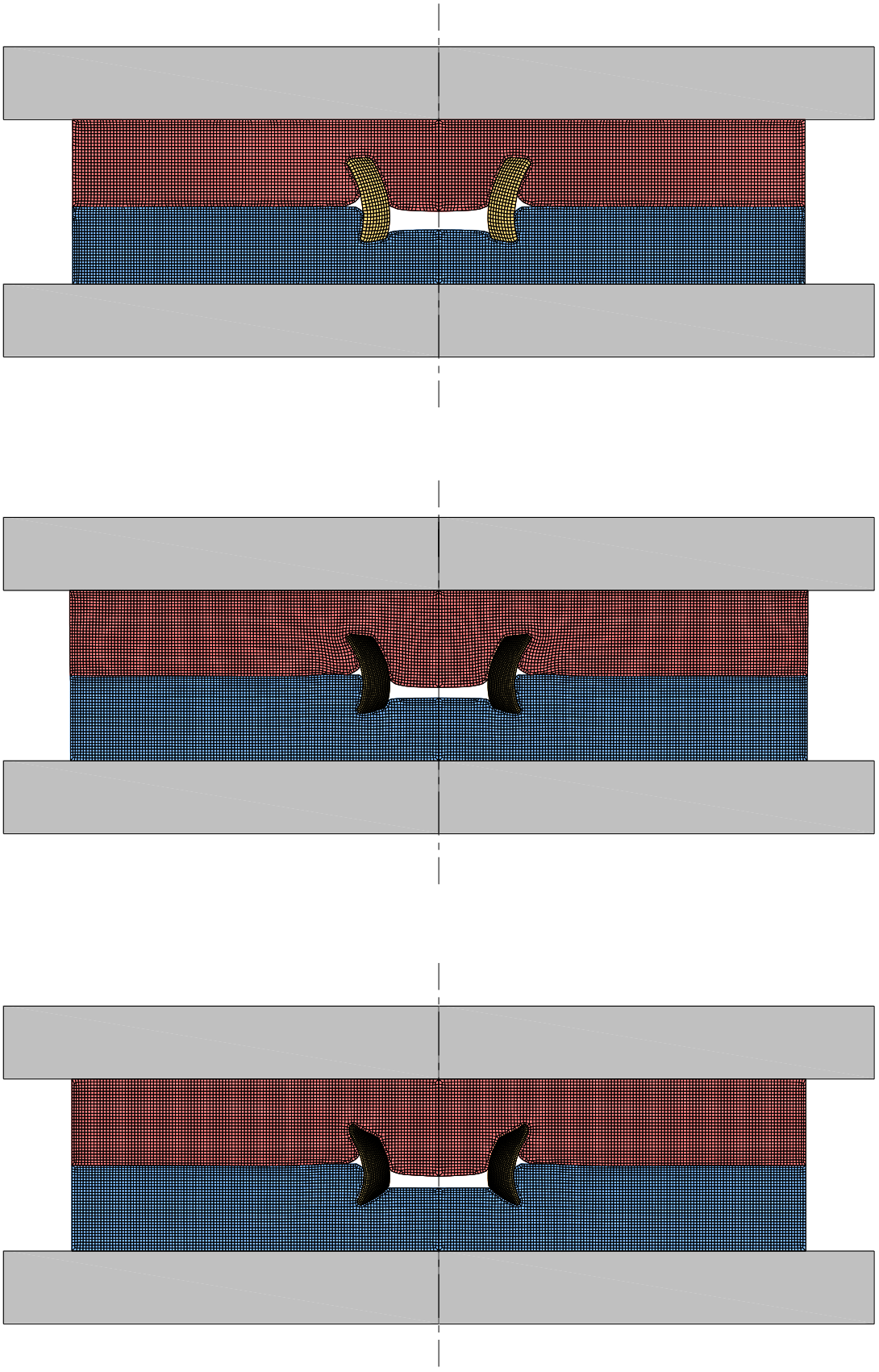

Figure 34. Finite element models of DSSPR with 2mm depth flat-bottom hole of AA5754-H111 aluminum and PVC sheets with AISI 304 stainless-steel rivets with h_0= 8 mm and chamfered angle of α= 60º (top) α= 45º (middle) and α= 30º (bottom) in both sides.

The chamfered angle sensitivity analysis yielded similar results to those obtained in similar material joints and were not, therefore, discussed in this section.

Additionally, the use of a rivet with distinct chamfered angles ($\alpha_{Al} = 30º$; $\alpha_{PVC} = 60º$) was also simulated and experimentally tested under the context of this study to assess if it could further benefit the performance and symmetry of the joint, by promoting the form-closing mechanism present in conventional DSSPR and absent in the proposed variant. The visual results of the mentioned configuration are presented below.

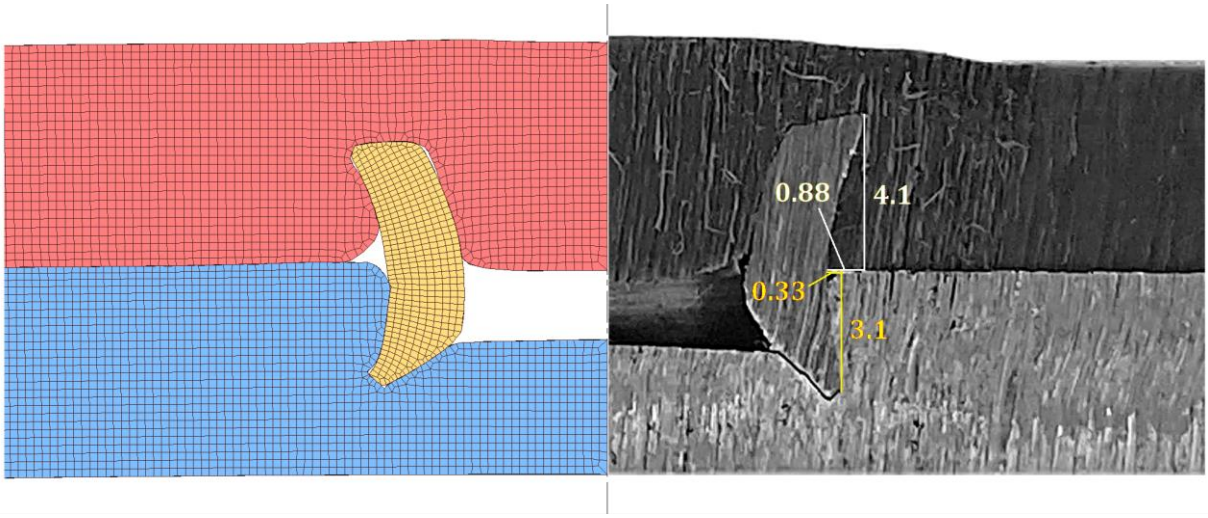

Figure 35. Finite element models of DSSPR with 2mm depth flat-bottom hole of AA5754-H111 aluminum and PVC sheets with AISI 304 stainless-steel rivet with h_0= 8 mm and chamfered angles with α_{Al}= 30º, α_{PVC}= 60º

In this configuration, an interlocking of 0.33 mm was measured in the aluminum sheet while an interlocking of 0.88 mm was measured in the PVC sheet, meaning the form-closed mechanism acted in the joint and complemented the force-closed mechanism. The performance of this variation will be analyzed and compared in the following section with the case where a regular rivet with chamfered angles of 45º was used.

The evolution of the riveting force with displacement was also retrieved from these experimental tests and were compared with the respective finite element models. Despite the introduction of the flat-bottom hole and the force-closing mechanism associated, the maximum force peaked at roughly 50 kN, similarly to the conventional DSSPR dissimilar material sheet joining. The force peaking at a lower displacement value was the only relevant difference and was justified by the existing smaller free height of the rivets that were placed inside the flat-bottom holes.

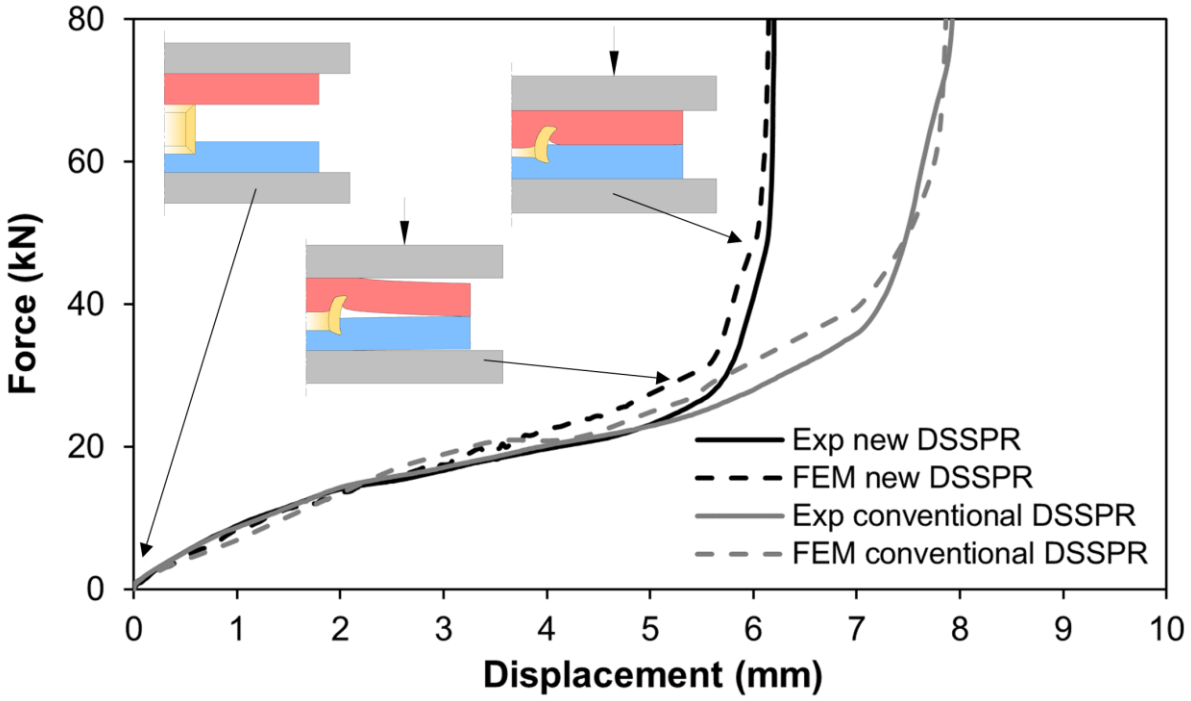

Figure 36. Experimental and finite element predicted evolution of the riveting force with displacement for the DSSPR with a 2mm depth flat-bottom hole of AA5754-H111 aluminum and PVC sheets with AISI 304 stainless-steel rivets with h_0= 8 mm and a chamfered angle α= 45º.

6.3 Destructive tests: comparative performance and discussion of proposed variants

From a development standpoint, it was considered relevant to assess the performance of the variants analyzed as a group to establish a direct comparison of the benefits and disadvantages when comparing to the standard joint results in dissimilar materials. The conventional application of DDSPR was only used as reference to these variants, since it was expected that the performance of the joint would be determined by the material with the least mechanical strength, in this case being the PVC, which would promote the separation of the joint in a prominent manner when compared to the aluminum sheet. This implied that the shear strength of the joint in dissimilar connections would be around the same value obtained in the monolithic PVC sheets shear test of around 2.5 kN. This deduction was later proven correct.

Regarding the two-stroke DSSPR variation, considering the reliable relation of the ratio between shear and peel forces of approximately 6 to 10 throughout the destructive tests in monolithic materials, it was expected that the ratio would maintain its consistency, yielding the same outcome for dissimilar materials. For that reason, only shear tests were carried to evaluate performance of the joint and it was considered relevant to compare the performance of the joint produced in dissimilar materials with the results from similar sheet materials.

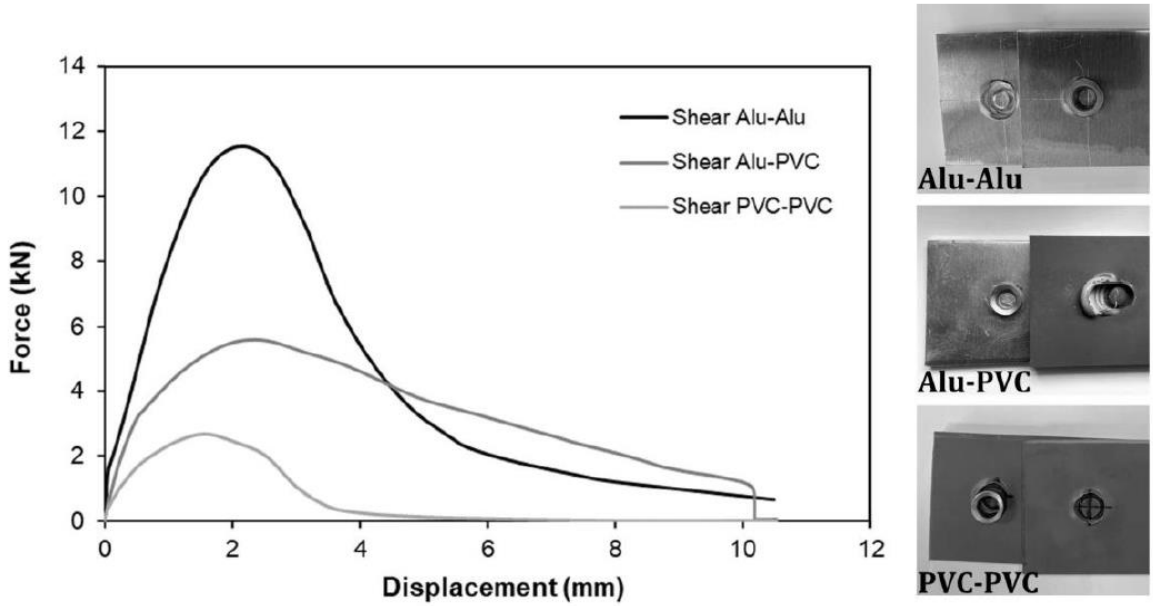

Figure 37. Experimental evolution of the destructive shear test force with displacement for the AA5754-H111-PVC joints (rivets with h_0= 8mm and α=45º) produced by two-stroke DSSPR. Results for the similar AA5754-H111 and PVC joints are provided for reference purposes. Photographs on the right display the shear test specimens after separation.

In terms of destructive testing performance in the aluminum sheets joining [2], the joint withstood a shear-shear force of approximately 11 kN,, comparable to a SPR joint [17], and a critical peel load of approximately 1.2 kN, which is comparable to the peel strength observed in clinched joints [18] and in

SPR joints [19] .Additionally, as discussed previously, the joint in polymer sheets reached a critical shear load of 2.7 kN.

Regarding the dissimilar material joint, this comparative test allowed to conclude that the maximum shear strength was between the values of the monolithic materials, reaching a value of approximately 5.5 kN. This result was attributed to the fact that the separation of the joint was being caused by a different deformation mechanism associated with material displacement of the PVC sheet caused by the rivet, where ridges alongside the groove were formed, as shown in the detail above.

For the performance analysis of DSSPR assisted with a flat-bottom hole, it was considered relevant to assess the sensitivity of the joint to the different angles tested and consequently the degree of interlocking achieved. In that scope, the graphic below gathers the results from destructive tests for the cases of conventional DSSPR and DSSPR with flat-bottom holes, with a symmetrical rivet ($\alpha_{Al} = \alpha_{PVC} = 45º$) and with a two-angle chamfered angle rivet ($\alpha_{Al} = 30º$; $\alpha_{PVC} = 60º$). Destructive peel tests were once again conducted to assess their influence in the performance of the joint.

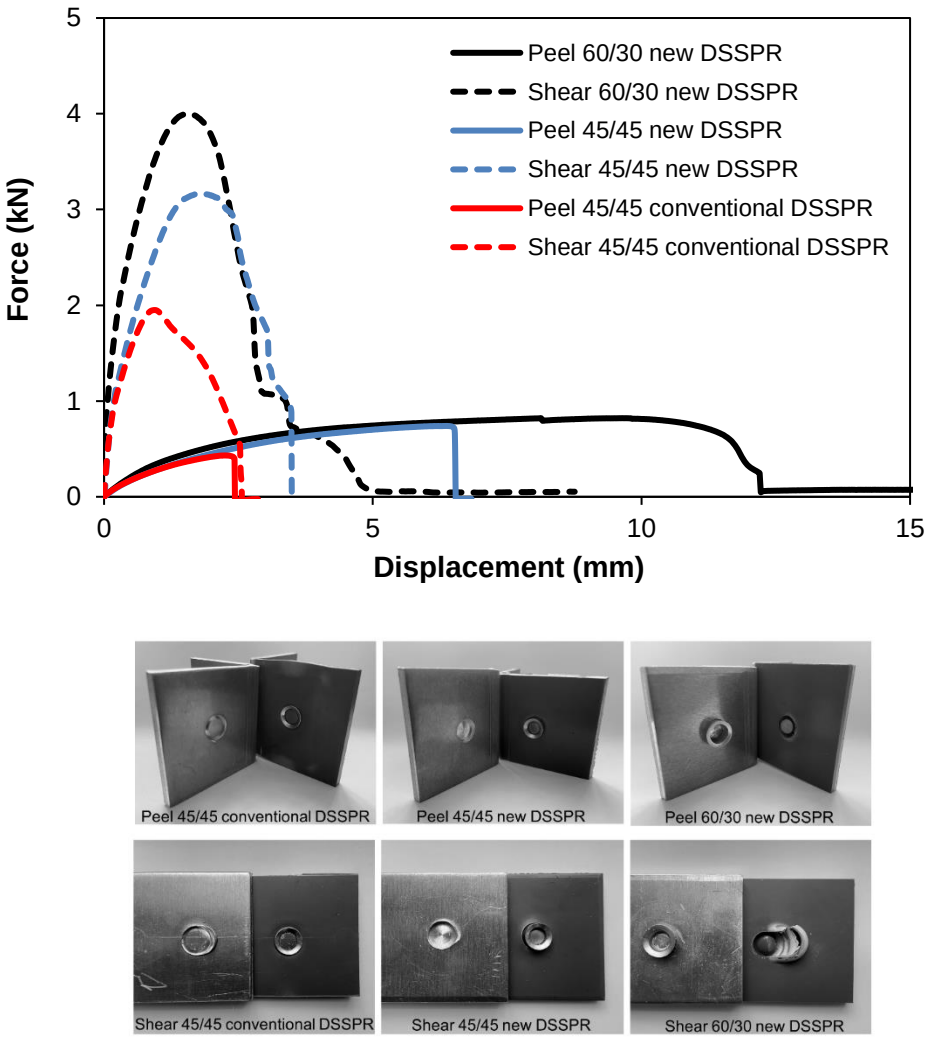

Figure 38. Experimental evolution of the destructive shear and peel tests force with displacement for the AA5754-H111-PVC joints produced by conventional DSSPR and DSSPR with 2mm flat-bottom holes with rivets with h_0= 8mm and both chamfered angles α=45º and two-angle rivets with α_{Al}= 30º, α_{PVC}= 60º. Photographs below display the shear test specimens after separation.

As depicted in Figure 38, the conventional application of DSSPR using a rivet with chamfered angles α= 45º generated the lowest performing joint in both tests, peaking at approximately 2 kN in shear and 0.5 kN in peel. Those results allowed to not only set the comparative performance of DSSPR with a flat-bottom hole, but also provided relevant insights regarding performance improvement associated with the firstly presented variant of double-stroke DSSPR, confirming the prediction made previously, that the joint would sustain a relatively similar maximum load to the one occurring in PVC monolithic material sheet joints.

As for the results obtained in the DSSPR joints with flat-bottom hole test subjects, it was observed that the joints significantly outperformed conventional DSSPR in both shear and peel tests.

Regarding shear resistance, DSSPR with a flat-bottom hole using rivets with α= 45º sustained a solicited load of 3 kN while the joint using different chamfered angle rivets with $\alpha_{Al} = 30º$ and $\alpha_{PVC} = 60º$ sustained a maximum load of 4 kN. This result was attributed to the observed and discussed combined action of the interlocking and friction on the outer rivet face contact with the sheet's slot, which delayed detachment of the rivet by shear.

Concerning peel resistance of the joint, greater values were once again obtained for the joints produced by the new DSSPR with two-angle chamfered angle rivets. The increase in performance was however observed in the total amount of displacement that the joints can safely withstand before critically failing, while the maximum force values were very similar. The increase in displacement was once again justified by the combined effect associated with the interlocking and friction present.

In conclusion regarding the scope of the proposed variant solutions, both presented overall positive improvements in terms of performance of the DSSPR joint. Comparatively, double-stroke DSSPR yielded better results than DSSPR with a flat-bottom hole. Nonetheless, this does not dismiss the potential application of the latter, as different advantages may be drawn from both. Considering an industrial perspective, both solutions proved the ability to solve potential positioning issues of the rivet, with the disadvantage of adding steps to the process. On one hand, implementing the double-stroke solution would require implementation of an additional stage and tool to the process, directly increasing the joint's associated costs and cycle time, while on the other hand, the flat-bottom hole solution would require a preparation process to one of the sheets to produce the flat-bottom hole, which would imply an increase in costs of the joint. The potential selection of the variant should, therefore, vary depending on the specifications of the application and available processes, that are the prepondering factors considered to significantly impact the direct costs of the joint.

7. Potential applications of DSSPR

The investigation developed during this work allowed to expand the knowledge of the technology of Double-sided self-pierce riveting (DSSPR), resulting in a more concrete perspective of what the implementation of the process at an industrial scale would look like. Although the experimental testing involved small sized specimens of materials, the detailed insights and data collected regarding the technical parameters and behavior of the process, provided confidence in the ability to transfer those results to specific industrial applications.

DSSPR is undoubtedly a comparable solution to SPR, that simultaneously differentiates itself in terms of potential applications, given the ability to perform mechanical joints of larger thickness components, comprising a vast range of geometries and materials. In that sense, a joint involving a circular profile and a sheet (or plate) made of dissimilar materials (Figure 39), is utilized, as an example, to illustrate how flexible and vast is the range of applications.

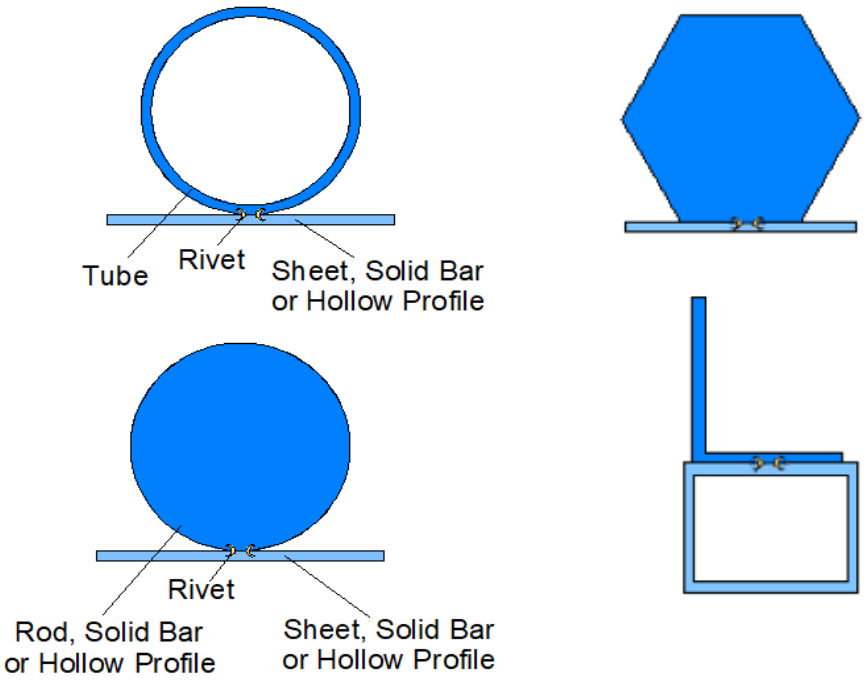

Figure 39. Examples of potential applications of DSSPR in different geometries.

On the other hand, provided that DSSPR is limited in terms of application in very thin sheets, there is a solid understanding of the parameters and variables of the process and its components that would allow the technology to be introduced in thin geometric features where SPR, flow drill screws and welding techniques are used. Although this work does not cover thickness variations of materials to be joined, parallel works were under development involving DSSPR in 1.5mm thick aluminum sheets (Figure 40), proving conceptually the potential implementation of the technology in features and components with geometries often used in the automotive and lightweight structures industries. This is easily understood,

since the DSSPR process parameters can be scaled to be applied to very thin sheets, although realistically the rivet cannot be so small because it will introduce some difficulties during manufacturing and/or positioning.

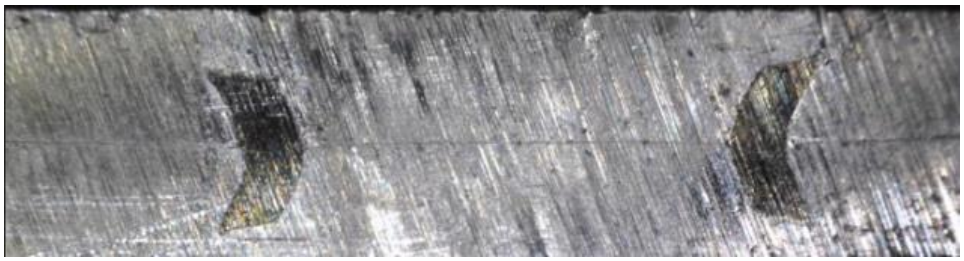

Figure 40. Experimental cross-section of DSSPR in 1.5 mm thick aluminum sheets.

Considering contemporary lines of production, where joining processes, (from welding to SPR) are often automated processes, DSSPR would only be a competitive technology if it could operate under the same conditions. This was considered an attractive aspect of DSSPR, since current (and even more simple) tooling used in SPR could easily be adapted to DSSPR, with the advantage of requiring access to only one side of the components to be joined together. One challenging aspect related with the flexibility of positioning and rivet feeding would, however, arise if not for the process variants proposed for dissimilar materials, which are considered very relevant from an industrial perspective, as they posed potential solutions to this challenge. Without them, and as an example, standard DSSPR would not be applicable to a platform with a robotic arm capable of riveting in multiple positions since it would not be able to feed a rivet between the two components to be joined and/or correctly hold in position. This represented a potential constraint to the technology, since the automated platform would have to strictly operate horizontally, and with lower velocities to allow for the placement of the rivet in between the geometries.

In this context, the proposed variant of a flat-bottom hole in one of the sheets would increase the flexibility of the process regarding positions in which the operation could be performed since the rivet would be physically constrained and positioned by the flat-bottom hole. Although this variant would require an additional drilling operation on the sheet, implying an increase in cycle time of the overall joining process, the consistency and quality of the joints would significantly improve due to the inherent benefits of using the flat-bottom hole as previously discussed, and would simultaneously facilitate the positioning, alignment and feed of the rivet.

Regarding the proposed double-stroke variant, the cycle time of the operation would in theory increase since two operations including one tool substitution would be required. On the other hand, the use of a conventional riveting machine, similar to the ones shown in Figure 41, could easily be adapted to perform the first and second strokes provided the correct tool adaptations are implemented. This solution would likewise benefit the positioning of the rivet and the flexibility in which the process could operate, while potentially providing a better performing joint.

Figure 41. Self-pierce riveting manual (left) and automatic (right) machines.

Additionally, the double stroke in DSSPR provides a unique opportunity to extend the range of potential applications. For instance, a hybrid mechanical joining element combining a rivet used in DSSPR in one side and another element like a fastener or a pin on the other could be created. This concept would potentially provide an alternative to current existing cases like the one shown in Figure 42, where a fastener is joined to a sheet or surface by means of stud-welding. Figure 42a (right) illustrates a specific example where these types of hybrid mechanical/welded joints are used in a 3 mm stainless steel sheet. As illustrated in Figure 42b, a fixture with a rivet could be used instead, avoiding subjecting the material to intense thermal cycles caused by welding that change the material properties and can create other drawbacks, while having the potential to be utilized to produce these types of joints in dissimilar material combinations. Furthermore, given the small dimension of the rivet, a potential weight reduction could be achieved and considering the comparative simplicity of the DSSPR riveting process, an increase in the assembly rate of these fixtures could be possible.

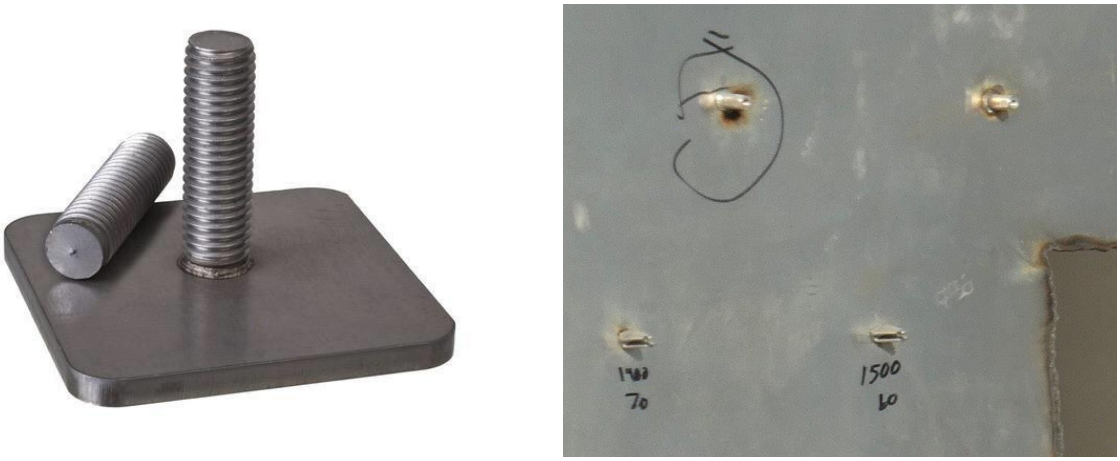

a)

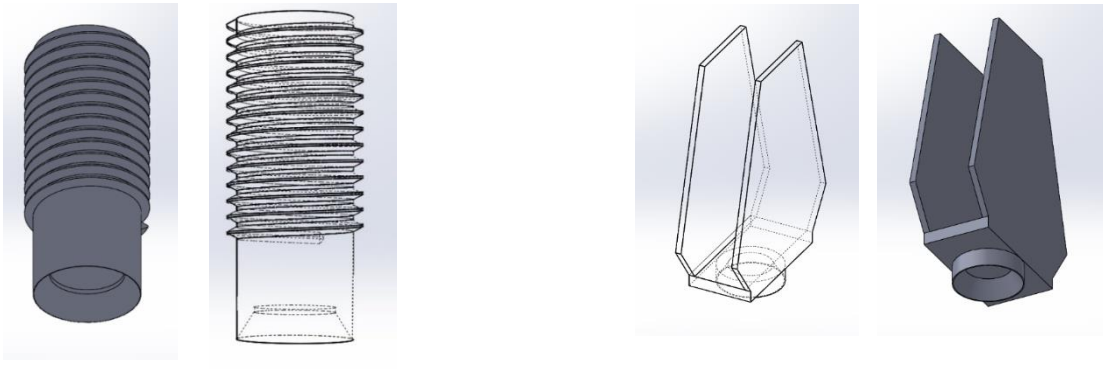

b)

Figure 42. a) Stud-weld example (left) and application (right); b) CAD models of hybrid riveting fastener (left) and pin fixture (right).

8. Economic viability of DSSPR

In the current state of the DSSPR technology, evaluating the economic viability in detail is a difficult task, since tangible applications and process structuring are key elements for this evaluation that are not yet fully defined. In this scope, only a qualitative evaluation is performed based in information found regarding the topic considering similarities drawn from analogous technologies like SPR.

A crucial aspect to assess cost effectiveness relates directly with the components' process operating costs. Regarding SPR, costs associated with rivets may range from 17€ to 58€ per 1000 rivets. Given its simple geometry, DSSPR rivets would require even simpler manufacturing operations of extrusion and forming. In fact, the symmetry and simplicity in these rivets may translate in simpler and more cost-effective manufacturing processes, increasing DSSPR's competitiveness. The second economic influencing factor affecting manufacturing costs is material usage. Establishing material costs is however strongly correlated with the application and process, which determines the geometry and amount of material required for the rivets. In this sense, it would be relevant to establish a cost comparison between DSSPR and SPR rivets for an identical application. As an example, assuming a joint between two 1.5mm thick sheets, from the experimental knowledge of this work, a DSSPR rivet with an initial diameter $\emptyset_0$ of 4mm and initial thickness t_0 of 0.5mm would be able to produce a joint, whereas the same joint made with SPR would require a more complex rivet of the same material with an initial diameter $\emptyset$ of 4mm, the same initial thickness and a length of 8mm [20] . Given the similar geometries of both rivets and based on the above-mentioned example, its intuitively possible to assume that the volume of DSSPR rivets is lower than that of SPR rivets, directly implying a lower mass and overall weight of the component. This weight reduction is beneficial not only in terms of material costs per rivet but also in terms of joint performance as weight reduction of the assemblies is a crucial industrial optimizating aspect. As shown in the figure below, consumables are responsible for more than half of the costs associated with SPR, so the predicted lower costs of DSSPR rivets present a great industrial opportunity in terms of economic competitiveness [21].

Lastly, tooling and energy consumption were considered relevant in terms of the economic assessment. At the present moment, tool costs of DSSPR equipment were estimated to be similar to the costs associated with SPR equipment. Briskham et al [21] and HE et al [7] performed a comprehensive economic analysis of SPR and other processes, where equipment cost, maintenance and labor costs were estimated for specific cases. Arguably, DSSPR was predicted to generate costs similar to those described in the papers mentioned.

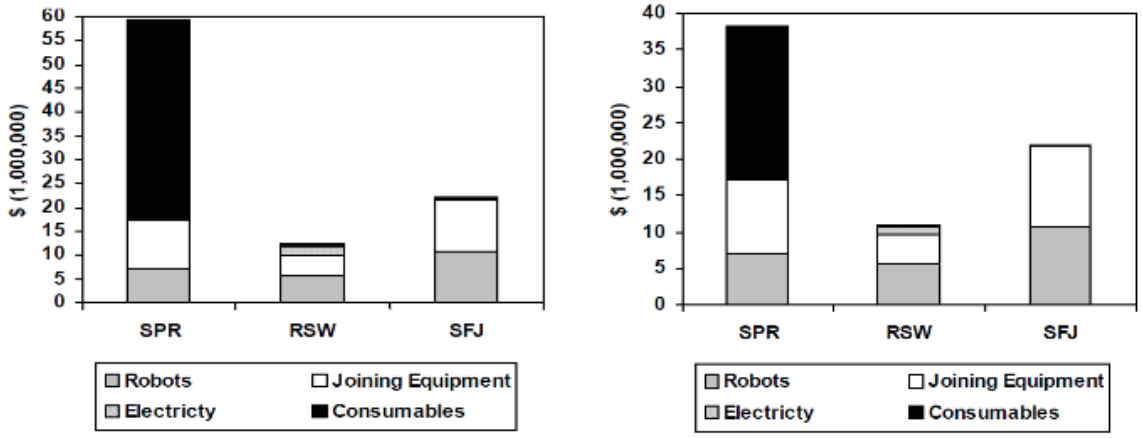

Figure 43. Comparison of cost differences for SPR, RSW and SFJ *[21]* associated with a) a production line with a volume of 35000 units/year running for 10 years b) a production line with a volume of 35000 units/year running for 5 years.

9. Perspectives of future developments

The work developed and presented thus far provided concrete insights of DSSPR regarding its mechanical feasibility, behavior and performance with polymers and dissimilar materials. Its development also allowed to push for process variants that not only inherently improve the quality of the joint but also carve a path towards its industrial implementation in cases where conventional solutions are limited by either materials or geometries.

With the knowledge acquired and potential demonstrated throughout DSSPR's development, perspectives for future developments are here proposed to further fuel and validate DSSPR as a competitive and viable industrial solution.

In terms of the technology itself, more specifically the rivets used, it was identified a series of optimization studies regarding their geometry. These studies include the deeper analysis of the interaction and respective influence between the rivet's initial thickness (refer to right image of Figure 44), height, and diameter to improve its weight-performance ratio. Additionally, the introduction of geometric features like grooves and notches in the rivet needs also to be considered since it is a study worth pursuing in terms of force and process performance optimization.

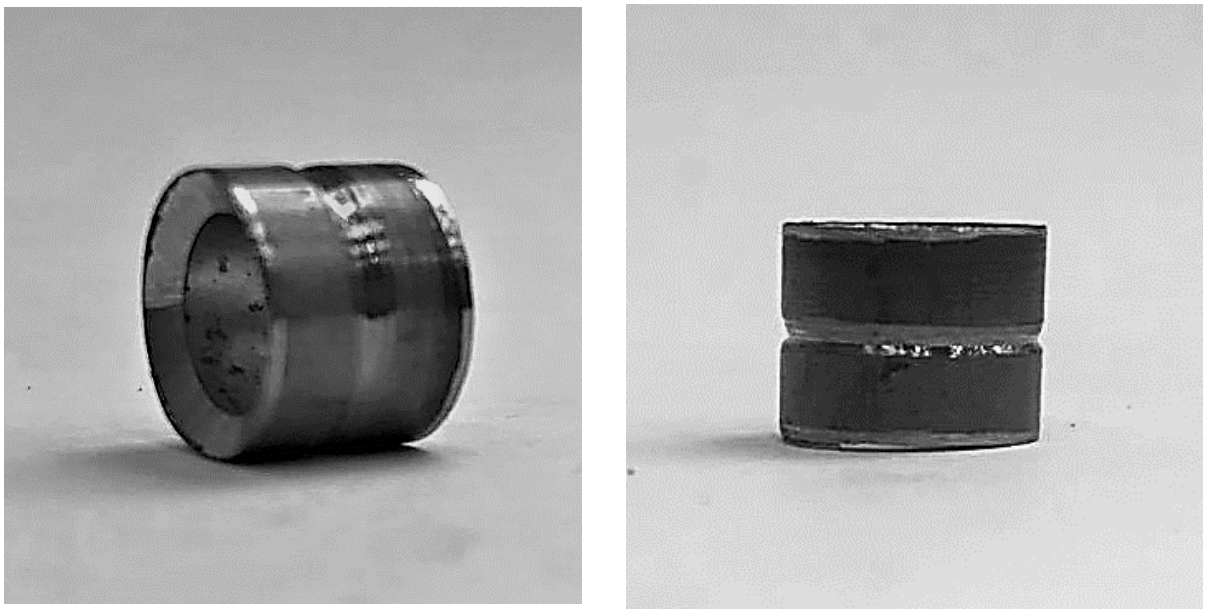

Figure 44. DSSPR rivet with circular groove.

In the same topic, material selection studies could also be conducted with the intent of expanding applications in terms of specific material property requirements, and additional weight-performance optimizations. The figure below depicts as an example a joining test conducted using a copper rivet to join two PVC sheets, that would be useful for guaranteeing electrical conductivity in polymeric materials.

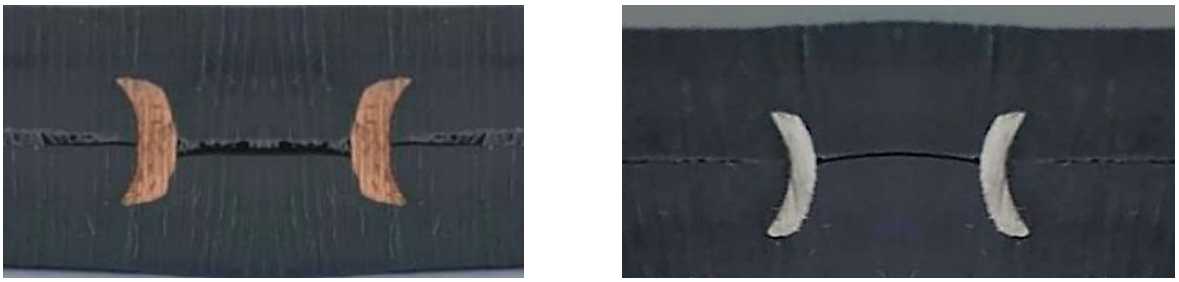

Figure 45. DSSPR of PVC sheets using a copper rivet (left) and a AISI 304 stainless-steel rivet with 1mm thickness (right)

Simultaneously, expanding the materials and geometries of the components to be joined should benefit DSSPR, as it would increase its application range while potentially promoting further process optimizations and variations. In that context, given a justifiable material selection, implementing DSSPR complemented with, for example, adhesive bonding or any other reasonable process could propel the technology in terms of performance and joint specification requirements. For safety reasons, some applications may demand the combined use of DSSPR and adhesive bonding to ensure a completely tight seal between the geometries assembled.

Finally, additional performance studies, particularly in fatigue are considered necessary and relevant to better understand failure mechanics and behaviors of DSSPR while providing a comparative fatigue performance to other conventional processes. This analysis should be of great relevancy, allowing a more realistic prediction of the behavior of the joint during its service life, along with non-destructive real time testing techniques.

To conclude, implementing DSSPR with dedicated equipment in a realistic context needs to be followed to better understand the complexity and technical requirements regarding tools and equipment essential for a large-scale industrial implementation. Developments associated with this approach should provide better understanding of the challenges and opportunities of this joining technology, and to fully determine its efficiency and both fixed and variable costs of the DSSPR process.

10. Conclusion

The investigation carried in this thesis successfully established and extended the potential of Double-sided Self-pierce Riveting both in terms of material range and in terms of industrial applications and implementation. The already established knowledge regarding the application of this technology in metals [2] paved further developments by identifying key parameters and variables related with the geometry of the rivets and with the deformation mechanics involved. The introduction of DSSPR in polymers was followed naturally, given the promising results, and already identified potential of joining different types of materials and even dissimilar materials, through an invisible joint without any protrusions.

The work developed in polymers proved its relevancy by confirming the implementation of DSSPR in materials with reduced mechanical strength, and exceeded expectations given the complex interaction between the polymer and the steel rivets, with very distinct properties. The characteristic elastic behavior of the PVC sheets soon introduced difficulties to the process in terms of instabilities associated with lack of friction between the sheets and the compressive plates and allowed to conclude that a better control of the process was required. Regardless, the sensitivity analyses conducted to the rivet's geometric variables yielded coherent and comparable results with the ones obtained in metals, suggesting a successful implementation of DSSPR in polymers.

With the success and knowledge gathered, the final proposition of this thesis intended to evaluate the feasibility of implementing DSSPR in dissimilar materials. This application represented a last hurdle to the technology in this work, as it was one of its main premises. Based on the interactions observed in the PVC sheets, the joining of dissimilar materials was expected to be a more difficult task. Initial results did in fact substantiate such expectation, since the produced joints lacked the ability to effectively join both sheets due to the asymmetrical piercing of the rivet in each component, justified by the difference in mechanical strengths of both materials. Despite the less satisfactory results, the existing confidence in DSSPR fueled the search for meaningful solutions to bypass the challenges present in dissimilar material joints, and two variant solutions were proposed: two-stroke DSSPR, and DSSPR assisted with flat-bottom holes. As discussed, both solutions successfully and significantly improved the generated joint's performance by allowing a more symmetrical piercing and better interlocking of the rivet in both sheets. Ultimately, both variants not only improved the joining by DSSPR of dissimilar materials, but also provided meaningful strategies to implement the technology at an industrial scale.

As a final remark, Double-sided Self-pierce Riveting still has a great range of developments to go through before being acknowledged as an alternative to conventional solutions, as discussed in chapters 7,8 and 9. In that sense, an additional purpose for this body of work was identified: to provide enough confidence, enthusiasm and curiosity pertaining this technology, in hopes of inspiring future works and its eventual implementation.

Bibliography

1. **Meschut G., Janzen V. , Olfermann T.** Innovative and Highly Productive Joining Technologies for Multi-Material Lightweight Car Body Structures. *Journal of Materials Engineering and Performance.* 2014, 23, pp. 1515–1523.

2. **Alves L.M., Afonso R.M., Martins P.A.F.** Double-sided self-pierce riveting. *The International Journal of Advanced Manufacturing Technology.* 2020, 108, pp. 1541–1549.

3. **Salamati M., Soltanpour M., Fazli A., Zajkani A.** Processing and tooling considerations in joining by forming technologies; part A-mechanical joining. *The International Journal of Advanced Manufacturing Technology.* 2019, 101, pp. 261–315.

4. **Laurence, C.** New crews cut weight when joining parts and sheets of metals. *Machine Design.* 26 de May de 2016.

5. **Aslan F., Langlois L., Balan T.** Experimental analysis of the flow drill screw driving process. *The International Journal of Advanced Manufacturing Technology.* 2019.

6. **He, X.** Clinching for sheet materials. *Science and Technology of Advanced Materials.* 2017, pp. 381-405.

7. **He X., Pearson I., Young K.** Self-pierce riveting for sheet materials: State of the art. *Journal of Materials Processing Technology.* 2008, pp. 27-36.

8. **Kato K., Okamoto M., Yasuhara T.** Method of joining sheets by using new type rivets. *Journal of Materials Processing Technology.* 2001, pp. 198-203.

9. **Alves L.M., Afonso R.M., Martins P.A.F.** Double-Sided Self-Pierce Riveting of Polymer Sheets. *The International Journal of Advanced Manufacturing Technology.* 2020, Vol. 3.

10. **Alves L.M., Nielsen C.V., Martins P.A.F.** Revisiting the fundamentals and capabilities of the stack compression test. *Experimental Mechanics.* 2011, 51, pp. 1565-1572.

11. **ISO 12996.** Mechanical Joining – Destructive Testing of Joints – Specimen Dimensions and Test Procedure for Tensile Shear Testing of Single Joints. 2013.

12. **ISO 23598.** Mechanical joining of sheet materials — Destructive testing of joints — Specimen dimensions and procedure for mechanized peel testing of single joints. 2021.

13. **Nielsen C.V., Zhang W., Alves L.M., Bay N., Martins P.A.F.** *Modelling of thermo-electro-mechanical manufacturing processes.* London : Springer-Verlag, 2013.

14. **Alves L.M., Silva F.L.R., Afonso R.M., Martins P.A.F.** Joining sheets to tubes by annular sheet squeezing. *Int J Mach Tools Manuf.* 2019, 143, pp. 16-22.

15. **Alves L.M., Afonso R.M., Pereira P.T., Martins P.A.F.** Double-Sided Self-Pierce Riveting of Dissimilar Materials. *International Journal of Advanced Manufacturing Technology.* 2021, pp. 1-9.

16. **Alves L.M., Afonso R.M., Pereira P.T. , Martins P.A.F.** Double-Sided Self-Pierce Riveting with Flat-Bottom Holes: A Feasibility Study. *Production Engineering.* 2021 (Submitted).

17. **He X, Pearson I, Young K.** Self-pierce riveting for sheet materials: state-of-the-art. *J Mater Process Technol.* 2008, 199, pp. 27-36.

18. **Zhang Y., He X., Wang Y., Lu Y., Gu F., Ball A.** Study on failure mechanism of mechanical clinching in aluminium sheet materials. *Int J Adv Manuf Technol.* 2018, 96, pp. 3057–3068.

19. **X. He, B. Xing.** The Ultimate Tensile Strength Of Coach Peel Self-Piercing Riveting Joints. *Strength of Materials.* 2013, Vol. 45, 3, pp. 386-390.

20. **Atlas Copco.** Selecting rivet-size application correctly. [Online] [Cited: May 15, 2021.] https://www.atlascopco.com/en-us/itba/expert-hub/articles/correct-rivet-size.

21. **Briskham P., Blundell N.,Han L., Hewitt R. , Young K.** Comparison of self-pierce riveting, resistance spot welding and spot friction joining for aluminium automotive sheet. *SAE Technical Papers.* 2006.